Offshore Low-trophic Aquaculture in Multi-Use Scenario Realisation

Grant agreement number: 101094065
Topic: HORIZON-MISS-2021-OCEAN-04-01
Starting date: 1 January 2023
Duration: 48 months

D3.1
Title: Data on farming productivity for different scenarios

Date of delivery:
31.12.2024

Organization name of lead participant for this deliverable:
Aarhus University

"Funded by the European Union, grant agreement NO 101094065. Views and opinions expressed are however those of the author(s) only and do not necessarily reflect those of the European Union or CINEA. Neither the European Union nor the granting authority can be held responsible for them."

Dissemination level		
PU	Public, fully open	x
Sen	Sensitive, limited under the conditions of the grant agreement (only for members of the consortium, incl the Commission Services)	

Deliverable number:	D.3.1
Deliverable title:	Data on farming productivity for different scenarios
Work package:	3
Lead participant:	Aarhus University

Authors		
Name	Organisation	E-mail
Antonio Agüera Garcia*	Institute of Marine Research	antonio.aguera@hi.no
Marie Maar*	Aarhus University	mam@ecos.au.dk
Johannes Pein	Hereon	johannes.pein@hereon.de
Charlotte Clubley	Aarhus University	cclubley@ecos.au.dk
Jonne Kotta	University of Tartu	Jonne.kotta@sea.ee
Janus Larsen	Aarhus University	janus@ecos.au.dk

*corresponding authors

Keywords
Production potential, environmental conditions, ecosystem models, dynamic energy budget, siting.

Review History				
Date	Version	Review Author	Organisation	E-mail
Dec 13. 2024	1	Øivind Bergh	Institute of Marine Research	Oeivind.bergh@hi.no
Dec. 16. 2024	1	Jun She	DMI	js@dmi.dk
Dec. 16. 2024	1	Øivind Strand	Institute of Marine Research	oivind.strand@hi.no

"Funded by the European Union, grant agreement NO 101094065. Views and opinions expressed are however those of the author(s) only and do not necessarily reflect those of the European Union or CINEA. Neither the European Union nor the granting authority can be held responsible for them."

Executive Summary
This document provides an overview of the datasets generated in Task 3.1 when applying the 3D ecosystem models and the box models at the different pilot areas. Here we provide a summary of the methodology: models applied, scenarios run, outputs and justification. Moreover, we provide also a description of the data sets contents including metadata. This deliverable is an ongoing work that will be updated during the project and reported again as part of D3.2 on ecosystem services, as that deliverable involves this same model runs while focusing on a different output. This dataset will be transferred to WP5 to be added to the OLAMUR data portal and used in WP2 micro-siting approach.

Indhold

"Funded by the European Union, grant agreement NO 101094065. Views and opinions expressed are however those of the author(s) only and do not necessarily reflect those of the European Union or CINEA. Neither the European Union nor the granting authority can be held responsible for them."

1. Introduction

The aim of this deliverable was to provide data sets of production capacity of low trophic aquaculture generated in Task 3.1. The data sets were used to demonstrate the efficiency of co-use scaled farming scenarios in offshore wind farms (OWF) and Integrated Multi-Trophic Aquaculture (IMTA) represented by the chosen pilots (WP1). This task used local high-resolution 3D ecological modeling of the pilot sites (SCHISM for pilot A and FlexSem for pilot B,) and box farm model for pilot C. The ecosystem models were coupled with existing Dynamic Energy Budget Individual Based population Models (DEB-IBM) for blue mussels, and in pilot C also for rainbow trout, whereas new models were developed for the seaweed sugar kelp and *fucus*. The models were used to assess farm-scale spatial production patterns. The output of these models was validated against the data gathered in the pilots (T1.4) and oceanographic monitoring data from WP4 and/or monitoring stations. These models linked local environmental conditions with the physiological performance of the crop to allow estimations of spatial and temporal variability of the crop status. Further, the developed models were used to compare the potential of the different pilots and relate that to their environmental particularities and their co-use in different farming scenarios including estimates of production carrying capacity. These data sets will also provide information for the development of tools for site selection (T2.3) and microsite selection within the co-use zone (T1.1 and T2.2).

Here we provide a summary of the methodology: models applied, validation, scenarios run, outputs, and justification. Moreover, we provide a description of the contents of the data sets including metadata. This deliverable is an ongoing work that will be updated during the project when new harvest data is becoming available in WP1 and reported again as part of D3.2 on ecosystem services, as that deliverable involves this same model runs while focusing on ecosystem services. This dataset will be transferred to WP5 to be added to the OLAMUR data portal and used in WP2 micro-siting tool.

2. Case study A: German Bight: Meerwind Süd-Ost

2.1. Description of modeling approach

To estimate aquaculture production in the area of case study A, we use an extension of the Semi-implicit Cross-scale Hydroscience Integrated System Model (SCHISM, Zhang et al. 2016) coupled via the Framework for Aquatic Biogeochemical Models (FABM, Bruggeman and Bolding, 2014) with the ECOSystem Model (ECOSMO, Daewel and Schrum 2013) modelling framework (in the following "SCHISM-FABM-ECOSMO", see Pein et al., 2021; 2024), which integrates existing DEB model of blue mussels (Maar et al., 2009; 2023). The modelling strategy for resolving the technical structures of the offshore wind farm in case study A is based on explicit resolution of the monopiles. The 80 monopiles of the wind farm *Meerwind Süd | Ost* were inserted into an existing model grid (Pein et al., 2023) and thus extend the high-resolution region north of Helgoland with minimum side lengths of the mesh cells of 2.5 m to the wind farm foundations. The aquaculture variables are initialized directly at the wind farm foundations.

"Funded by the European Union, grant agreement NO 101094065. Views and opinions expressed are however those of the author(s) only and do not necessarily reflect those of the European Union or CINEA. Neither the European Union nor the granting authority can be held responsible for them."

The modelling framework is based on the hydrodynamic core of the SCHISM model (Zhang et al., 2016). SCHISM solves the Reynolds-averaged Navier-Stokes equations on an unstructured grid and is characterised by robust and efficient solution algorithms that make it possible to calculate complex coupled models in model areas with sometimes very high resolution over relevant time periods. The proven ecosystem model ECOSMO (Schrum et al., 2006; Daewel and Schrum 2013) is coupled with SCHISM via the coupling interface FABM (Bruggeman and Bolding, 2014).

The integrated model system physics-ecology-aquaculture described here was developed during the reporting period based on the existing model framework SCHISM-FABM-ECOSMO and existing F90 and XML codes of blue mussel dynamics from other models (Maar et al. 2009, 2023). In order to be able to access the latest and most sophisticated SCHISM and FABM versions, further adjustments were made to the codes. The complete modelling framework physics-ecology plus DEB mussel model was run in a semi-coupled mode with mussel growth depending on the Chl *a* availability but with the depletion of Chl *a*. This approach was chosen to assess the growth and harvest potential at the site using different parametrization from the literature. For the default scenario exercise, namelist parameters reported by Maar et al. (2009) were adopted. The two-coupling with depletion of phytoplankton by the mussel is technically accomplished and will be presented in the next deliverable.

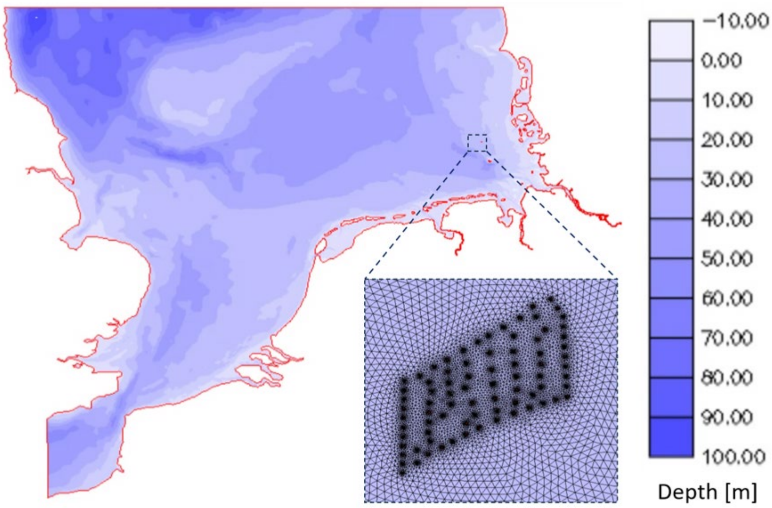

Figure 2.1. *Model domain used to simulate the physical-biogeochemical and DEB farm dynamics at offshore wind parm Meerwind (case study A).*

The model area of the southern North Sea and the German estuaries allows extensive flexibility in the choice of oceanic forcing (Fig. 2.1). Here, the physical re-analyses available via CMEMS based on the AMM15 model were used for the forcing of water levels, salinity, temperature and horizontal velocities. These data have hourly resolutions and are therefore tide-resolving. The atmospheric forcing is based on the re-analyses of the German Weather Service with the COSMO-EU model (Kaspar et al., 2020). The discharges of seven major rivers around the southern North Sea, including the Rhine, Ems, Weser and Elbe, were compiled from raw data

"Funded by the European Union, grant agreement NO 101094065. Views and opinions expressed are however those of the author(s) only and do not necessarily reflect those of the European Union or CINEA. Neither the European Union nor the granting authority can be held responsible for them."

from the Waterways Administration and processed data (kindly provided by S. van Leeuwen, NIOZ). The same applies to the nutrient concentrations of the contributories.

2.2. Model validation

The physical-biogeochemical coupled model, which serves as the basis for the coupling with the DEB model, was calibrated and validated for the year 2020. Figure 2.2 shows a comparison of the simulated concentration of suspended particles and the chlorophyll *a* (Chl *a*) concentration with satellite data of the coastal ocean available via CMEMS from 1 January 2020 (see product ID OCEANCOLOUR_NWS_BGC_HR_L3_NRT_009_203). The comparison shows that the model reproduces the magnitude of observed surface Chl *a* and represents a valid basis for estimating the nutrient flux between the physical-biogeochemical and the DEB model (Fig. 2.2). Here the average bias between satellite-observed and simulated Chl *a* was 1.36 mg m^{-3}. At Helgoland island, which is located 23 km south-east of the case study A site, the bias between model and observations was 0.12 mg m^{-3}. The DEB model will also be validated as soon as the field data of case study A from WP1 are available during 2025.

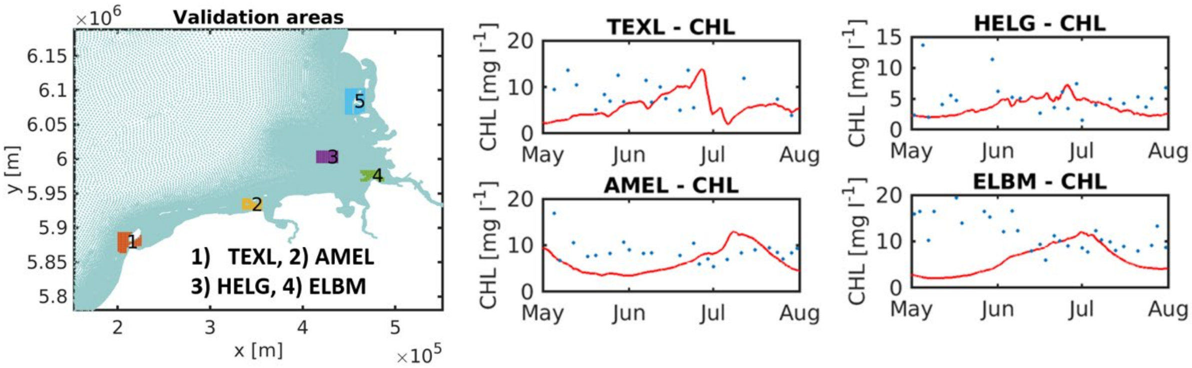

Figure 2.2. *Validation of simulated surface Chl a (red solid line) versus satellite observations (blue dots) at several stations across the model domain, where 1) Texel area, 2) Ameland area, 3) Helgoland area, 4) Elbe estuary mouth area.*

2.3. Run scenarios

Based on the SCHISM-FABM-ECOSMO outputs the Chl *a* flux in the farm area was estimated based on velocity fields and Chl *a* concentrations (Fig. 2.3). According to the illustration high Chl *a* fluxes occurred north of Helgoland island. Elevated Chl *a* fluxes were predicted also for the northern part of the Meerwind offshore wind park, whereas its south-western margins receive less Chl *a* forcing. In comparison with other coastal areas of the southern North Sea, the Helgoland area reveals relatively low Chl *a* concentrations (Fig. 2.2). Against this background the case study A site appears as an important benchmark to assess the feasibility of regions with relatively low primary producer concentrations for feasibility of aquaculture production.

"Funded by the European Union, grant agreement NO 101094065. Views and opinions expressed are however those of the author(s) only and do not necessarily reflect those of the European Union or CINEA. Neither the European Union nor the granting authority can be held responsible for them."

A modified parameterization was tested aiming to adopt katabolic rates from Buer et al., 2020 (see Fig. 2.1). The first parametrization (scenario 1) yielded a mussel harvest of up to 350 g/m² dry-weight (DW) (Fig. 2.4). The second parametrization (scenario 2) yielded a much smaller harvest of less than 50 g-DW m^{-2}. This result demonstrates the sensitivity of parametrization and the importance of comparison of simulated growth with field data from the case study site (WP1).

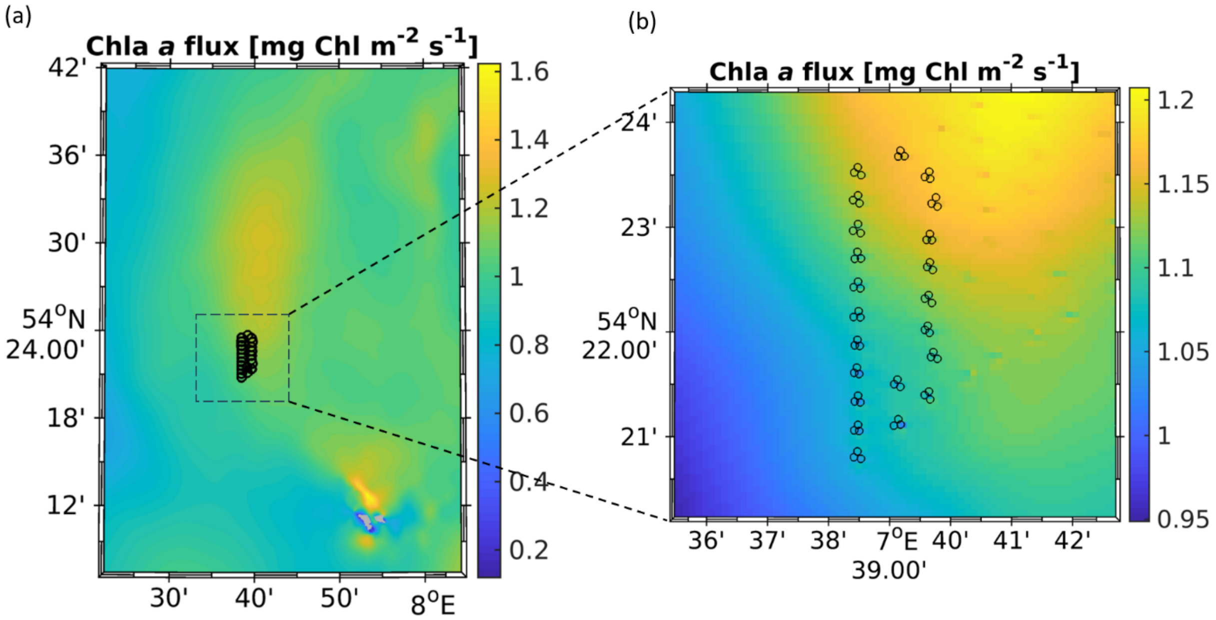

Figure 2.3. *(a) Simulated surface Chl a flux compiled from the coupled physical-biogeochemical model run during the second half of 2020. Helgoland island is indicated by grey surface in the south-eastern corner. (b) Zoom into the area demarked by the black dashed line in (a). The aquaculture farms are located at the western end of Meerwind süd OWF and indicated by black circles.*

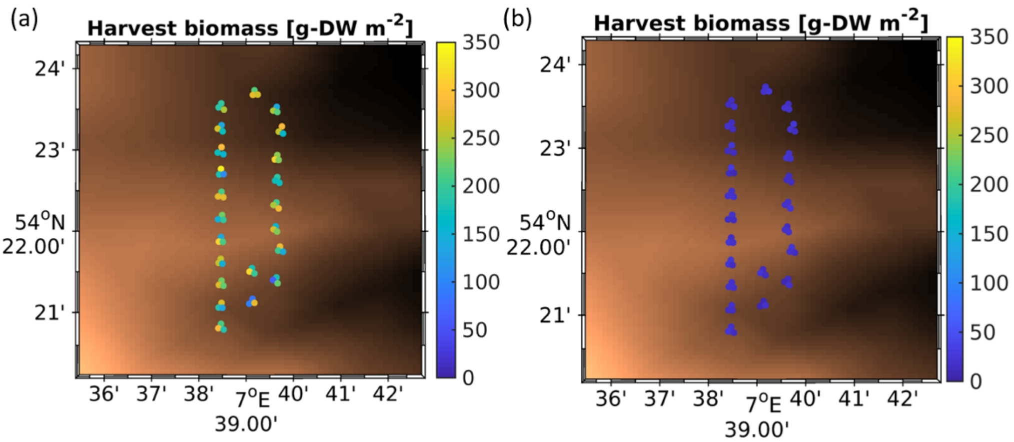

Figure 2.4 *Harvest biomass of blue mussel with parametrization referring to (a) scenario 1 and (b) scenario 2 against the background of local bathymetry (brownish colors).*

2.4. Description and metadata for produced dataset

The farm production data was saved in terms of daily mussel volume, number of mussels m^{-2} and mussel DW per individual at the locations where a farm was initialized. The harvest as g-

"Funded by the European Union, grant agreement NO 101094065. Views and opinions expressed are however those of the author(s) only and do not necessarily reflect those of the European Union or CINEA. Neither the European Union nor the granting authority can be held responsible for them."

DW m^{-2} can be estimated from the number of mussels multiplied by the individual DW. The farm locations are given in geographical coordinates. The data format is netcdf with dimensions spanned by the farm index and time. For each of the scenarios one netcdf file was saved.

3. Case study B: Danish Kriegers Flak

3.1. Description of modeling approach

3.1.1 Study area

Kriegers Flak is a shelf located in the Western Baltic Sea, where European energy company Vattenfall runs an offshore wind farm consisting of 72 turbines (area: 132 km^2; Figure 3.1.1). Within Kriegers Flak, a pilot farm site composed of four long lines, two with the blue mussel, *Mytilus edulis*, and two with the sugar kelp, *Saccharina latissima*, were deployed in November 2023 (kelp) and May 2024 (mussels) between monopiles in the south-western corner (Figure 3.1.1; WP1). Data on the biomass of mussels and kelp at the pilot farm from the first growth season have begun to be collected, with biomass measurements for kelp available for 16th April and 21st May 2024 (final harvest). Mussel biomass data is not yet available and final harvest will take place end of 2025. A second round of validation data for the second growth season (2024/2025) will be available next year.

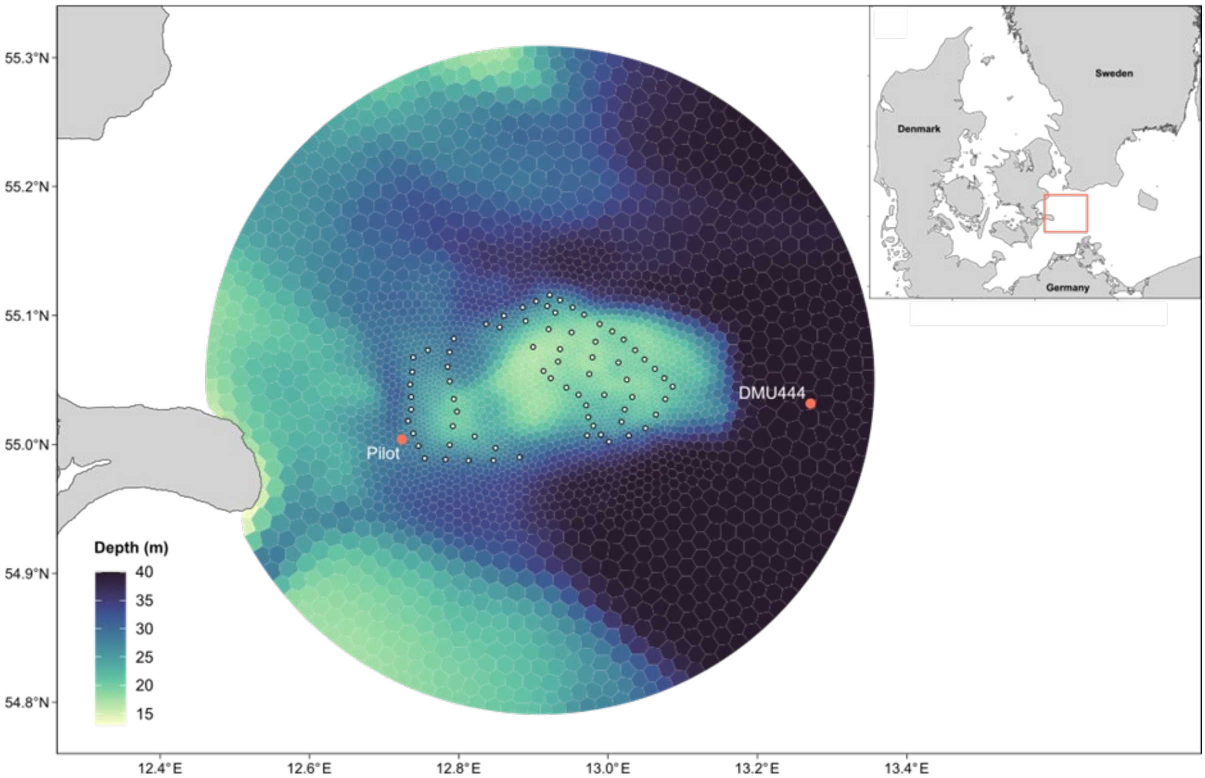

Figure 3.1.1. *Study area. The model domain showing bathymetry (m depth). White circles show the locations of the 72 wind farm pylons that make up Kriegers Flak offshore wind farm. Also shown is the location of the monitoring station DMU444, and the location of the pilot farm for mussel and kelp aquaculture (orange circles). Inset shows the location of Kriegers Flak in the Southern Baltic Sea (red box).*

"Funded by the European Union, grant agreement NO 101094065. Views and opinions expressed are however those of the author(s) only and do not necessarily reflect those of the European Union or CINEA. Neither the European Union nor the granting authority can be held responsible for them."

3.1.2 Model system

As a part of this work, the effects on the environment and the potential for multi-use of the Kriegers Flak offshore wind farm with aquaculture of mussels and kelp are being evaluated by dynamic models simulating the growth of these two species with the FlexSem model framework (https://marweb.bios.au.dk/flexsem). These models are fully coupled to a 3D biogeochemical model, which is one-way coupled to a hydrodynamic model. The nonhydrostatic hydrodynamic setup in FlexSem uses a computational mesh which varies in horizontal resolution from 343 m within the wind farm to 1,654 m in the area outside of the wind farm. The model has a circular open boundary broken only by the westernmost point of the island of Møn, Denmark. Open boundary conditions and initial fields for both hydrodynamics and biogeochemistry were interpolated from a previous run of the Inner Danish Waters. Maximum water depth in the model is 40 m, separated into 19 layers: seven 1 m depth layers in the upper 7 m, nine 2 m layers from 7-25 m and three 5 m layers from 25-40 m. The model has a total of 56,310 computational cells. Meteorological forcings were interpolated from WRF model version 3 output provided by the Danish Technical University (DTU). This included current wind turbines in the area and the associated wind wake. The physical effects from monopiles were added as drag and turbulent kinetic energy (Rennau et al. 2012). The model has a timestep of 120 seconds and was run for all of 2019.

3.1.3 Biogeochemical model

The biogeochemical model in FlexSem simulates changes in nutrients (NH_4, NO_3, PO_4), phytoplankton biomass, zooplankton biomass (meso- and microzooplankton), oxygen, detritus, and DON (labile and refractory dissolved organic nitrogen). The model estimates processes such as primary and secondary production, nutrient uptake, grazing, recycling of nutrients, excretion, respiration, growth, and mortality.

3.1.4 Mussel and kelp growth models

The biogeochemical model is two-way coupled to a DEB-IBM mussel growth model and a sugar kelp growth model. The mussel model is based on a previously published model (Buer et al. 2010, Taylor et al. 2021, Maar et al. 2023, 2024). The mussel model tracks the biomass (g-DW) and shell length (cm) of mussels over time and was initialised on 1st July and harvested on 31st December the next year (1.5-year growth period). The mussel model uses temperature, salinity, and food (phytoplankton microzooplankton, and detritus) as input from the biogeochemical model.

The newly developed sugar kelp model is based on a growth model described and parameterised by Holst et al. (in review), where growth of the standing crop of kelp (*M*, g-DW m line^{-1} day^{-1}) is described as a function of the daily total of global irradiation:

$$\Delta M = \left(\alpha \times S_f\right) \times M_{CH_2O} \times I_{abs} - (r \times M)$$

Where α is the quantum yield (CO_2 quantum^{-1}); fixed CO_2 contributes to kelp biomass as glucose at a rate of 6 CO_2 per $C_6H_{12}O_6$, with a molar weight M_{CH_2O} = 30 g mol^{-1}; I_{abs} is the daily total of light absorbed by the kelp canopy (mol PAR m^{-1} d^{-1}); r is the base respiration rate of kelp (0.01 g g-DW^{-1} d^{-1}; Holst et al. in review); and S_f is a salinity function describing

"Funded by the European Union, grant agreement NO 101094065. Views and opinions expressed are however those of the author(s) only and do not necessarily reflect those of the European Union or CINEA. Neither the European Union nor the granting authority can be held responsible for them."

the effect of sub-optimal salinity (S, psu) in the Baltic Sea area on kelp growth, based on that described by Maar et al. (2023):

$$S_f(\alpha) = \left\{1\ for\ S \geq 25; 1 + \frac{S-25}{18} for\ 16 \leq S < 25; \frac{S}{32} for\ S < 16\right\}$$

The kelp model tracks the biomass of kelp over time and was initialised on 1st January and harvested on 1st June. Later harvest was not possible due to settling of mussel spat on the crop at the study site.

3.2. Model validation

3.2.1 Validation of environmental parameters

3.2.1.1 Methods

Environmental observations from the DMU444 monitoring station (Figure 3.1.1) were extracted from the Danish National Database on Aquatic Monitoring (https://odaforalle.au.dk) for the year 2019 for model validation. We compared model outputs to *in situ* observations of surface temperature, surface salinity, surface nitrate, surface phosphate, surface Chl *a*, Secchi depth, and surface and bottom oxygen. Agreement between the model data and *in situ* observations was assessed by calculating Pearson's correlation coefficient (*r*) with a type II error of 5, normalised standard deviation (nSD), and a cost function (CF):

$$CF = \left|\frac{(\overline{m} - o)}{\sigma_o}\right|$$

Where $\overline{m}$ is the mean of model data, $\overline{o}$ is the mean of observational data, and σ_o is the standard deviation of the observational data (Radach and Moll 2006). The model performance can, according to the CF value, be good (CF < 1), reasonable (CF = 1-2), or poor (CF > 2; Eilola et al. 2011). Hence, the model results are interpreted as good if the model mean deviates with less than plus or minus one standard deviation from the observed mean.

3.2.1.2 Validation results

Model performance for ecological variables were all either 'good' or 'reasonable' as determined by the cost function (Table 3.2.1), with the exception of bottom oxygen concentration, for which there was also a low correlation with observations (Figure 3.2.1H; Table 3.2.1). This is likely due to too much mixing at the bottom layer in Spring. Surface values for temperature, nitrate, phosphate and oxygen showed the best agreement with observations across the calculated metrics (Figure 3.2.1A, C, D, G; Table 3.2.1). Model performance for Chl *a* and Secchi depth were both 'good', but model data did not significantly correlate with observations and both parameters were underestimated in winter months (Figure 3.2.1E, F; Table 3.2.1).

"Funded by the European Union, grant agreement NO 101094065. Views and opinions expressed are however those of the author(s) only and do not necessarily reflect those of the European Union or CINEA. Neither the European Union nor the granting authority can be held responsible for them."

Table 3.2.1. *Validation results of environmental parameters in Kriegers Flak. The results of Pearson's correlation tests (r), calculation of cost function (CF), and normalised standard deviation (nSD) between environmental parameters from the FlexSem model for Kriegers Flak and* in situ *observations from monitoring station DMU444.*

Parameter	*t*-value	DoF	*p*-value	*r*	R^2	*CF*	nSD
Surface temperature	11.56	20	2.63×10^{-10}	0.93	0.87	0.06	1.34
Surface salinity	2.60	20	0.017	0.50	0.25	1.04	2.97
NO_3	3.11	18	0.006	0.59	0.35	0.55	0.57
PO_4	5.66	18	2.28×10^{-5}	0.80	0.64	0.47	1.09
Chl *a*	1.28	18	0.217	0.29	0.08	0.11	2.01
Secchi depth	0.96	13	0.353	0.26	0.07	0.03	1.36
Surface O_2	7.48	21	2.38×10^{-7}	0.85	0.73	0.18	1.30
Bottom O_2	-1.63	5	0.163	-0.59	0.35	2.36	1.56

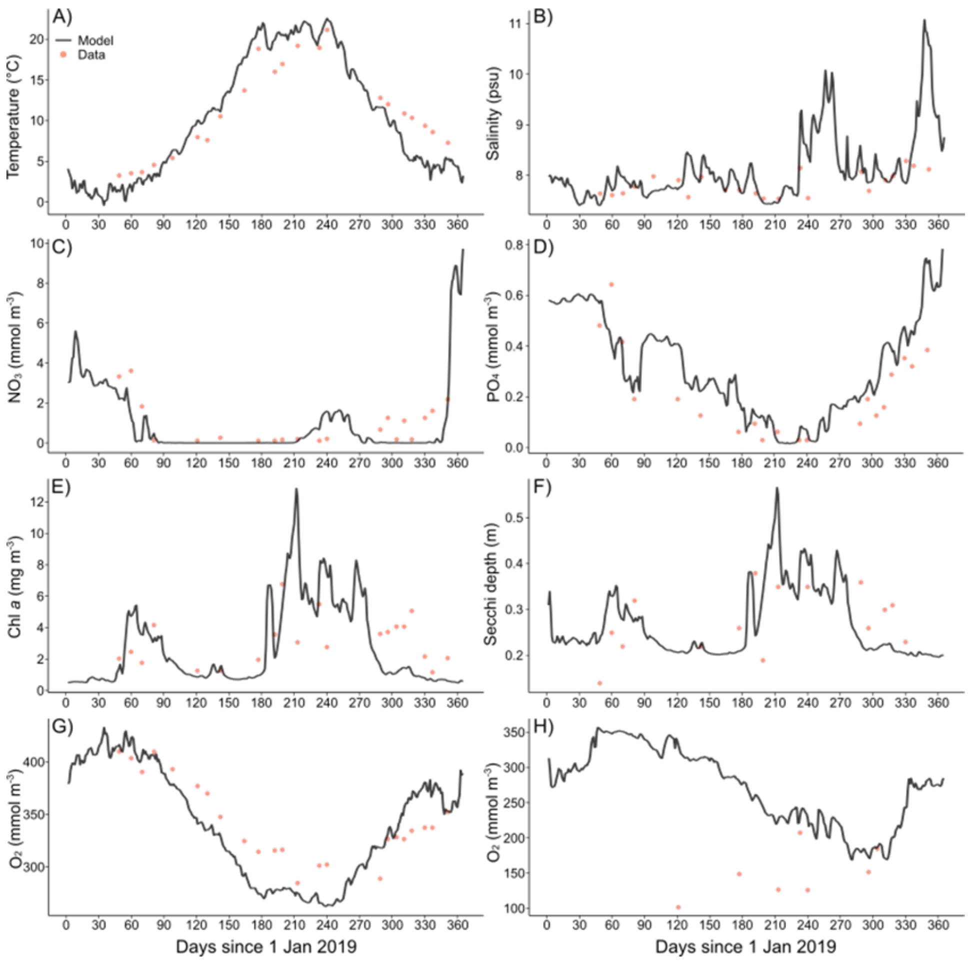

Figure 3.2.1. *Model calibration of water column properties at the monitoring station DMU444. A) Surface temperature (°C); B) Surface salinity (psu); C) Surface nitrate concentrations (mmol m*$^{-3}$*); D) Surface phosphate concentrations (mmol m*$^{-3}$*); E) Surface chl* a *concentrations (mg m*$^{-3}$*); F) Secchi depth (m); G) Surface oxygen concentrations (mmol m*$^{-3}$*); and H) Bottom oxygen concentrations (mmol m*$^{-3}$*).*

"Funded by the European Union, grant agreement NO 101094065. Views and opinions expressed are however those of the author(s) only and do not necessarily reflect those of the European Union or CINEA. Neither the European Union nor the granting authority can be held responsible for them."

3.2.2 Validation of biological parameters

3.2.2.1 Methods

Model results of kelp biomass were compared to measurements of kelp DW taken from the pilot farm (WP1). Average kelp biomass (g-DW per m of line) at 1 m depth on the 16th April 2024, and at 1 m, 3 m, 6 m and 15 m depth on the 21st May, was calculated from measurements of six individuals per depth (30 measurements total). Two values for average biomass were calculated for each depth on the two days: (i) the average biomass of kelp from a strain from Kiel, Germany, that had undergone salinity adaptation, (ii) the average biomass of kelp from a strain from Kiel, Germany, that not undergone salinity adaptation (WP1). Average biomass values were compared with model values from the day of measurement. Due to insufficient data from the pilot farms, no formal analyses of model performance for biological parameters were conducted. Mussel biomass data will become available in 2025.

3.2.2.2 Results for kelp

Model results of the kelp growth model showed a strong agreement with observations from the Kriegers Flak pilot farm across depth bands, falling within the standard deviation from the average biomass values in most cases (Figure 3.2.2). Kelp biomass was highest at 1 m and 3 m depths, decreasing with further increases in depth to produce very low values at 15 m in both the model and pilot farm observations. Kelp biomass was somewhat underestimated by the model at 15 m depth, likely due to a strong effect of light limitation within the model.

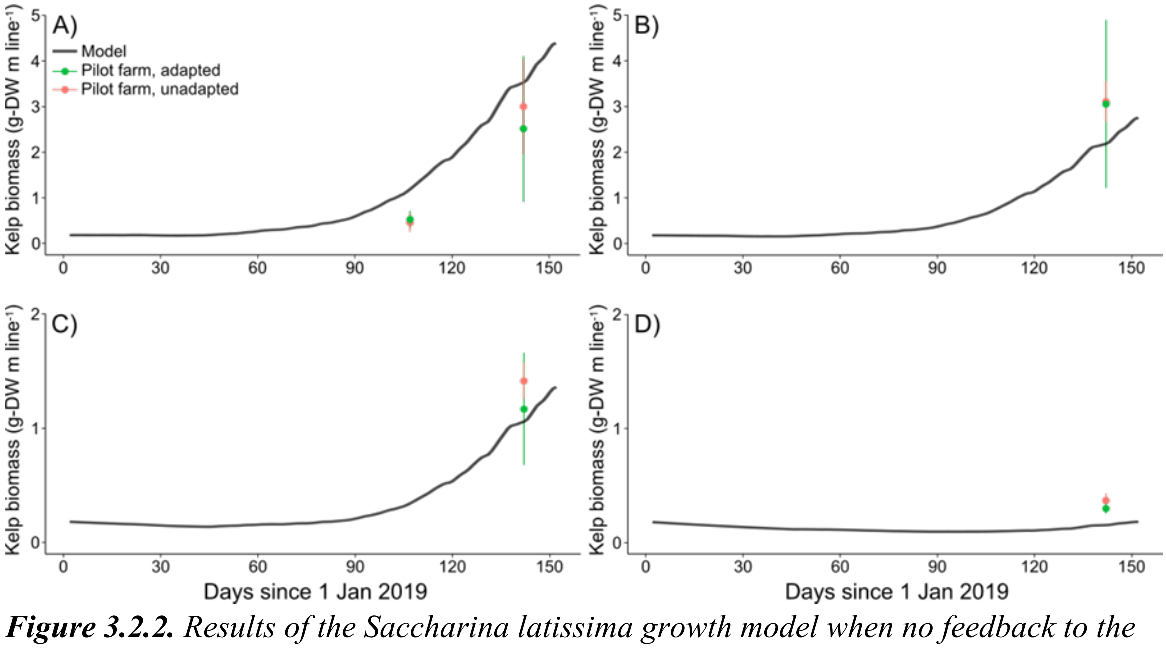

Figure 3.2.2. *Results of the Saccharina latissima growth model when no feedback to the biogeochemical model was included. Data represents the period 1 Jan 2019 – 1 Jul 2019 – the production period for* S. latissima *biomass. A) Kelp biomass at 1 m depth; B) kelp biomass at 3 m depth; C) kelp biomass at 6 m depth; D) kelp biomass at 15 m depth. Solid line shows the results of the model, whilst points show the average (± SD) of measurements taken from the pilot farm in Kriegers Flak, for kelp strains that have undergone salinity adaptation (green) and those that have not undergone salinity adaptation (pink).*

"Funded by the European Union, grant agreement NO 101094065. Views and opinions expressed are however those of the author(s) only and do not necessarily reflect those of the European Union or CINEA. Neither the European Union nor the granting authority can be held responsible for them."

3.3. Model scenarios

A number of steps were conducted in order to assess the harvest potential and suitability of locations within the Kriegers Flak wind farm for mussel and kelp aquaculture. First, the potential harvest of both species within the boundary of the wind farm (+ 200 m buffer) was screened based on the maximum food/nutrient fluxes, which assured a high food/nutrient supply and less risk of depletion, and the maximum growth of mussels and kelp (no depletion considered). Based on this screening process, a harvest potential score (ratio from 0 to 1) was estimated and used to place the mussel and kelp farms at the most optimal sites for assessment of production carrying capacity in two-way coupled runs with the biogeochemical model.

Screening of optimal sites. A model was run in which kelp and mussel farms were placed within every computational cell of the FlexSem model and no feedback to the biogeochemical model was included. In this way, farms in neighbouring cells do not influence each other through the depletion of nutrients/food and the maximum potential for growth of both species can be assessed. From the model output, harvest potential was assessed based on spatial variability in food and nutrient supply and the biomass of mussels and kelp at the ends of their respective production periods.

In the low trophic aquaculture farms, depletion of nutrients and food will occur to a variable extent dependent on the food/nutrient flux by advection. A higher food/nutrient flux will support a higher growth rate of the focal species, and therefore can be used as an indicator for farming potential. The daily average food flux (mg Chl *a* m^{-2} s^{-1}) for mussels from 1 – 5 m depth (chosen as mussels at the pilot farm are grown between 1.5 m and 5 m) was estimated by multiplying food concentration (mg Chl *a* m^{-2}) by the current speed (m s^{-1}). Values were averaged across time from 1st January – 31st December, representing the production period for mussel culture, to show spatiotemporal variability in food supply (Figure 3.3.1A). Similarly, the daily average nutrient flux (mmol N m^{-2} s^{-1}) from 0 – 15 m depth (depth of kelp cultivation at pilot farm) was estimated by multiplying DIN (mmol N m^{-2}) by the current speed. Values were averaged across time from 1st January – 1st June, representing the production period for kelp, to show spatiotemporal variability in nutrient supply (Figure 3.3.1B).

The maximum growth of mussels and kelp was calculated as the biomass of both species on their respective 'harvest' dates. For mussels, model values for biomass (g-DW) on the 31st December were summed from 1 – 5 m depth (Figure 3.3.2A). For kelp, model values for biomass (g-DW) on the 1st June were summed from 0 –6 m depth (Figure 3.3.2B). The biomass of kelp at depths greater than 6 m were excluded from the total biomass sum as values were negligible.

"Funded by the European Union, grant agreement NO 101094065. Views and opinions expressed are however those of the author(s) only and do not necessarily reflect those of the European Union or CINEA. Neither the European Union nor the granting authority can be held responsible for them."

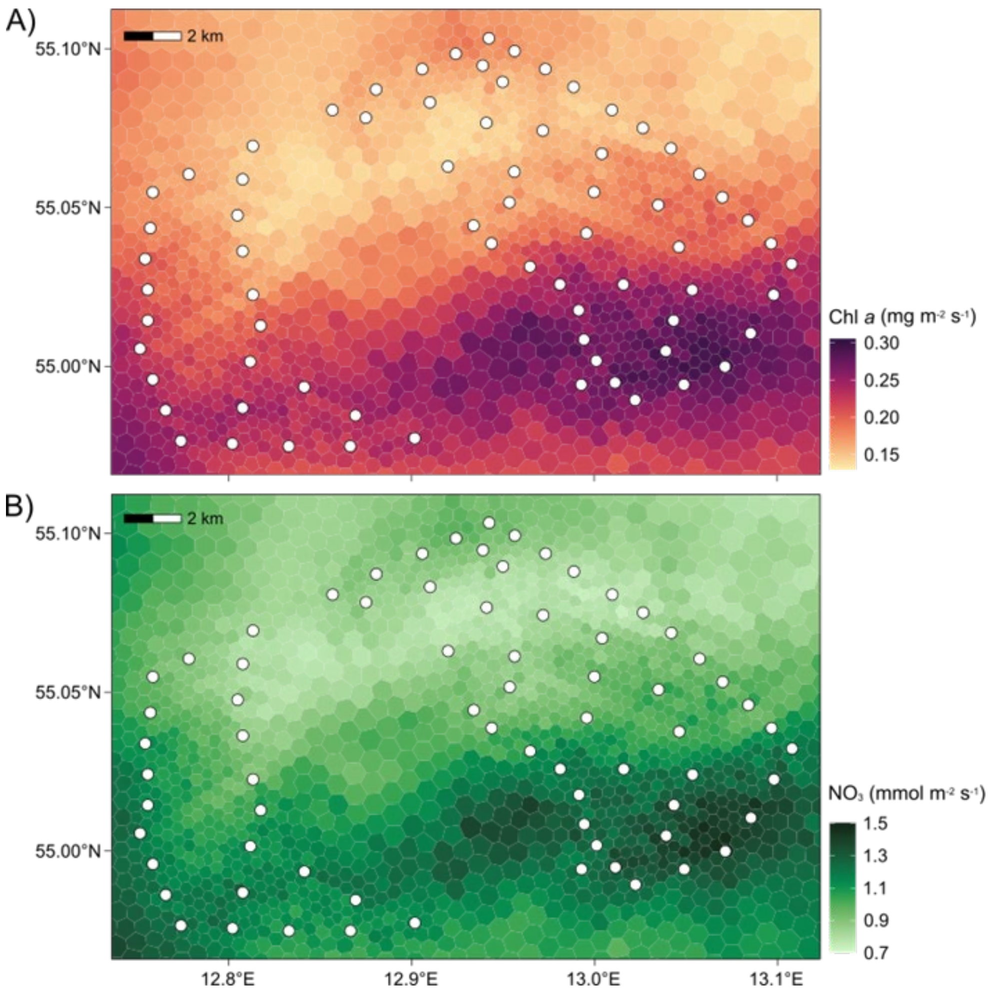

Figure 3.3.1. *Average food and nutrient flux within the Kriegers Flak offshore wind farm. A) Average food flux (mg Chl* a *m^{-2} s^{-1}) over the period 1 January – 31 December 2019. B) Average nutrient flux (mmol NO_3 m^{-2} s^{-1}) over the period 1 January – 1 June 2019. White circles show the locations of the 72 wind turbines within the offshore wind farm.*

"Funded by the European Union, grant agreement NO 101094065. Views and opinions expressed are however those of the author(s) only and do not necessarily reflect those of the European Union or CINEA. Neither the European Union nor the granting authority can be held responsible for them."

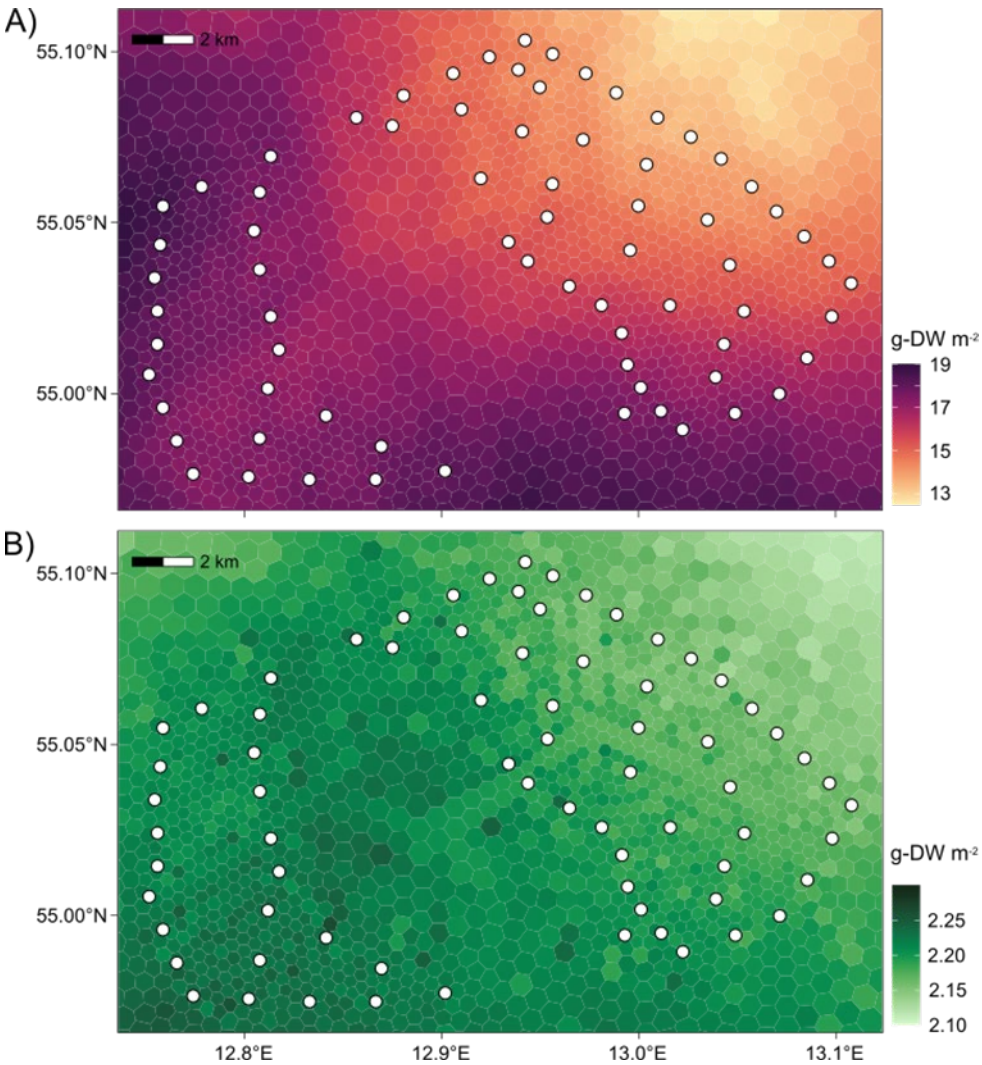

Figure 3.3.2. *Maximum potential biomass of mussel and kelp farms within the Kriegers Flak offshore wind farm.* ***A)*** *Maximum potential biomass (g-DW m^{-2}) of mussels at time of harvest (31st December).* ***B)*** *Maximum potential biomass (g-DW m^{-2}) of kelp at time of harvest (1st June). White circles show the locations of the 72 wind turbines within the offshore wind farm.*

<u>Harvest potential score.</u> Based on this screening process, a harvest potential score (ratio from 0 to 1) was created by summing the normalised food or nutrient flux and the normalised maximum growth of mussels or kelp, respectively, and re-normalising the summed value. This provided a 'harvest potential' score for each model cell within the wind farm. Cells above the 66th percentile were considered as the most promising sites for aquaculture (Figure 3.3.3).

"Funded by the European Union, grant agreement NO 101094065. Views and opinions expressed are however those of the author(s) only and do not necessarily reflect those of the European Union or CINEA. Neither the European Union nor the granting authority can be held responsible for them."

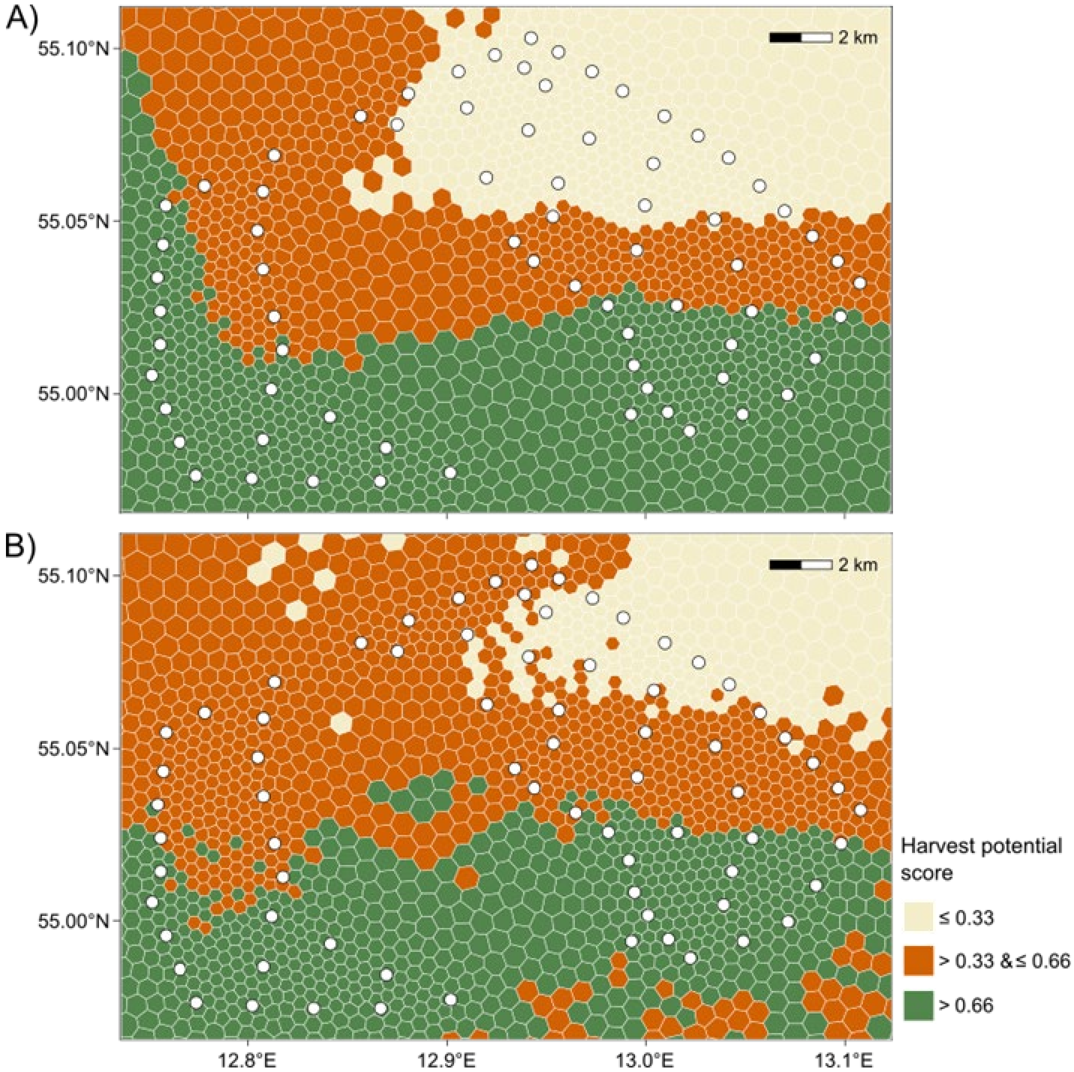

Figure 3.3.3. *Areas within the Kriegers Flak offshore wind farm with poor (yellow), medium (orange), or high (green) suitability for mussel and kelp aquaculture.* ***A)*** *Spatial variability in the harvest potential of mussels* ***B)*** *Spatial variability in the harvest potential of kelp. White circles show the locations of the 72 wind turbines within the offshore wind farm.*

To determine areas within the Kriegers Flak wind farm that are suitable for both mussel and kelp aquaculture, the harvest potential scores were cropped to just the areas of the pylons and model cells with a score of > 0.66 for both mussels and kelp were deemed to hold 'high' harvest potential for co-location, model cells with a combination of medium (> 0.33 & ≤ 0.66) and high (> 0.66) potential or solely medium potential across both species were deemed to hold 'medium' harvest potential for co-location, and model cells with a combination of medium and poor (≤ 0.33) or solely poor potential were deemed to hold 'poor' potential for co-location (Figure 3.3.4).

"Funded by the European Union, grant agreement NO 101094065. Views and opinions expressed are however those of the author(s) only and do not necessarily reflect those of the European Union or CINEA. Neither the European Union nor the granting authority can be held responsible for them."

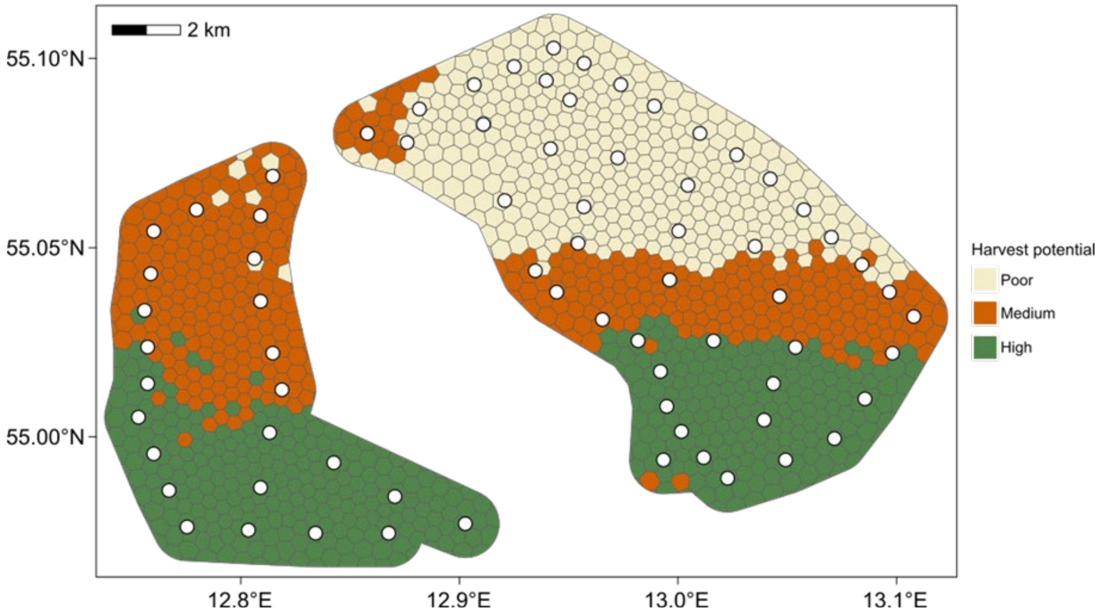

Figure 3.3.4. *Areas within the wind farm pylons of Kriegers Flak offshore wind farm with poor (yellow), medium (orange), or high (green) suitability for aquaculture of both mussels and kelp. White circles show the locations of the 72 wind turbines within the offshore wind farm.*

Production carrying capacity. Areas of high harvest potential for co-location of species were used to evaluate the effects of depletion and interactions between adjacent aquaculture farms on growth by fully two-way coupling the kelp and mussel farm models with the biogeochemical model. A number of scenarios were run, outlined in Table 3.3.1 and visualised in Figure 3.3.5, with increasing distance between neighbouring farms. Distance between farms was increased at intervals of 343 m, which was equivalent to the horizontal resolution of the computational mesh within the wind farm area.

Table 3.3.1. *Overview of model scenarios, with mussel and kelp farms placed at increasing distance from one another.*

Scenario	Description	Number of farms	Feedback to BGM	Mussel farm	Kelp farm
M0	Farm in all model elements (used to calculate harvest potential)	3391	×	✓	×
K0			×	×	✓
M1	Farm placed only in pilot farm location	1	✓	✓	×
K1			✓	×	✓
M2	Farms placed 343 m distant from one another	112	✓	✓	×
K2			✓	×	✓
M3	Farms placed 686 m distant from one another	55	✓	✓	×
K3			✓	×	✓

"Funded by the European Union, grant agreement NO 101094065. Views and opinions expressed are however those of the author(s) only and do not necessarily reflect those of the European Union or CINEA. Neither the European Union nor the granting authority can be held responsible for them."

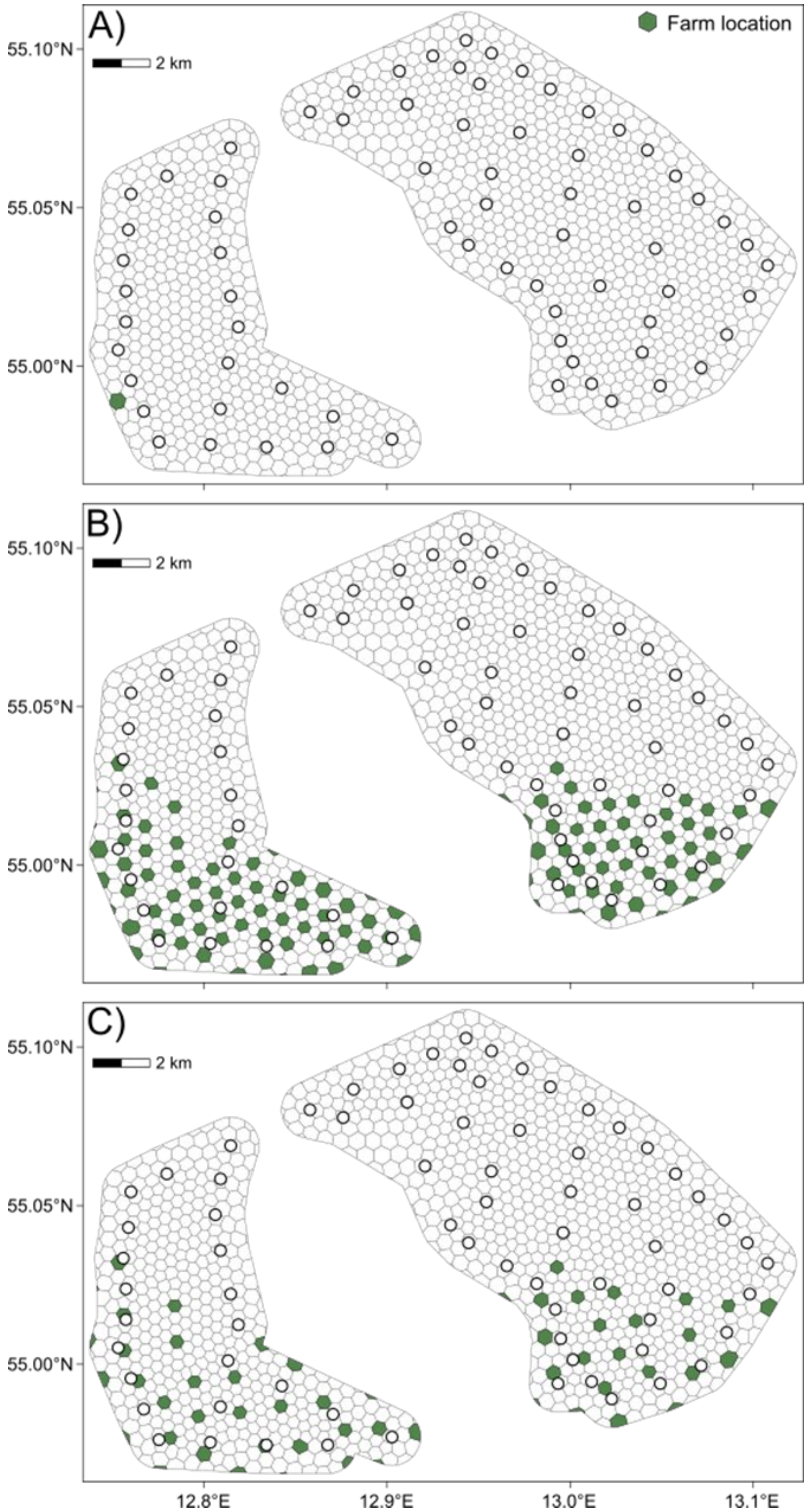

Figure 3.3.5. *Locations of mussel and kelp farms within the Kriegers Flak wind farm area in the different model scenarios. Green elements indicate a farm location. White circles show the locations of the 72 wind turbines within the offshore wind farm.* ***A)*** *Mussel and kelp farm location for scenarios M1 and K1. The farm is located in the model element corresponding to the location of the pilot farm at Kriegers Flak (WP1).* ***B)*** *Mussel and kelp farm locations for scenarios M2 and K2 (112 farms, 343 m distant).* ***C)*** *Mussel and kelp farm locations for scenarios M3 and K3 (55 farms, 686 m distant).*

"Funded by the European Union, grant agreement NO 101094065. Views and opinions expressed are however those of the author(s) only and do not necessarily reflect those of the European Union or CINEA. Neither the European Union nor the granting authority can be held responsible for them."

3.4. Description and metadata for produced dataset

3.4.1 Mussel farming productivity

The maximum potential biomass of mussels (g-DW m^{-2}) from 1 – 5 m depth at time of harvest (31st December) for scenario M0 (the screening scenario) is displayed in Figure 3.3.2A. At the time of harvest (31st December) mussel biomass from 1 – 5 m depth at the pilot farm location in Scenario M1 was 17.13 g-DW m^{-2} (Figure 3.4.1A). Average mussel biomass across farm locations at the time of harvest was 15.35 ± 0.54 g-DW m^{-2} for Scenario M2 (343 m distance between farms; Figure 3.4.1B) and 16.04 ± 0.57 g-DW m^{-2} for Scenario M3 (686 m distance between farms; Figure 3.4.1C).

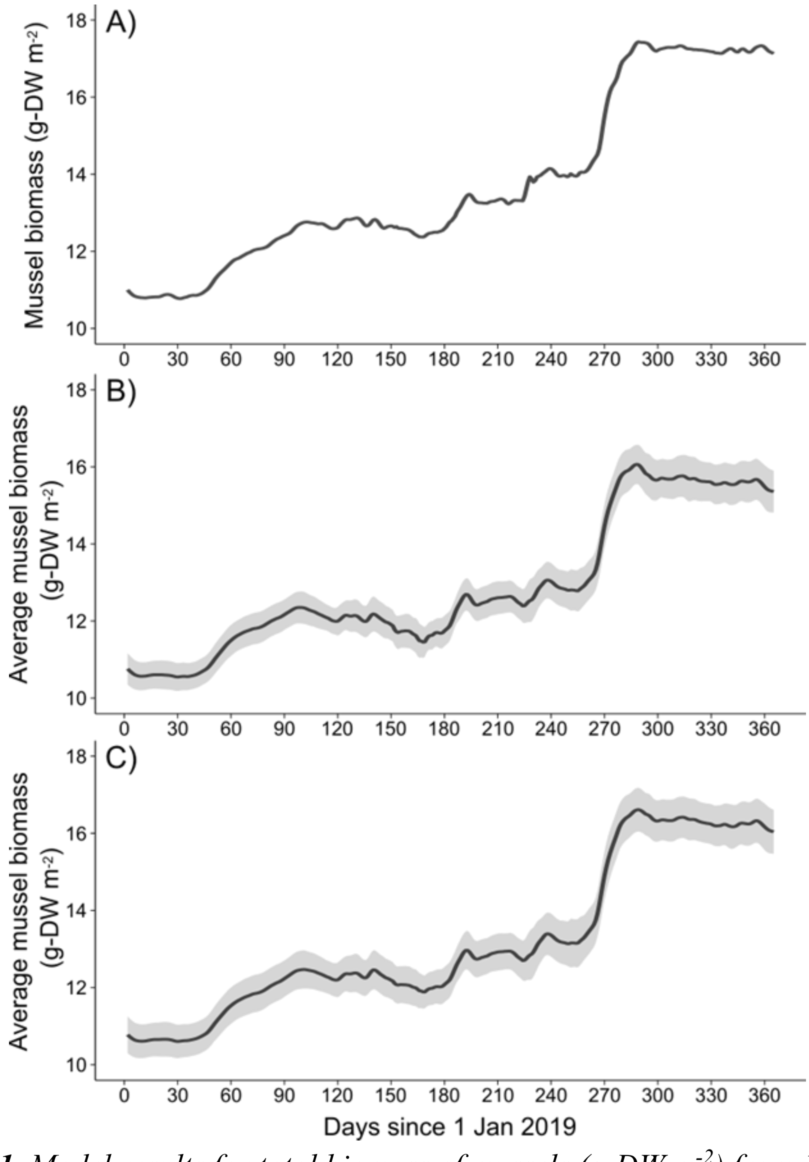

Figure 3.4.1. *Model results for total biomass of mussels (g-DW m^{-2}) from 1st January – 31st December for model scenarios M1, M2 and M3.* ***A)*** *Mussel biomass in scenario M1, where a single mussel farm was placed in the pilot farm location.* ***B)*** *Average mussel biomass of a single farm in scenario M2, where 112 farms were placed 343 m distant from one another.* ***C)*** *Average mussel biomass of a single farm in scenario M3, where 55 farms were placed 686 m distant from one another. In* ***B*** *and* ***C****, the shaded area indicates ± the standard deviation of the average value.*

"Funded by the European Union, grant agreement NO 101094065. Views and opinions expressed are however those of the author(s) only and do not necessarily reflect those of the European Union or CINEA. Neither the European Union nor the granting authority can be held responsible for them."

Mussel biomass (g-DW m^{-2}) per individual farm at the time of harvest was greater in scenario M3, where farms were placed 686 m distant from one another than scenario M2, where farms were placed 343 m distant from one another (Figure 3.4.2). This would suggest that when placed too close together adjacent mussel farms negatively interact with one another leading to a decrease in biomass. Mussel biomass in scenarios M2 and M3 was generally lower than for scenario M0, where there was no feedback (depletion) from the mussel model to the biogeochemical model. When mussel harvest data becomes available, the density of mussels per m of rope in the farm will be adjusted accordingly and this may increase the harvest potential.

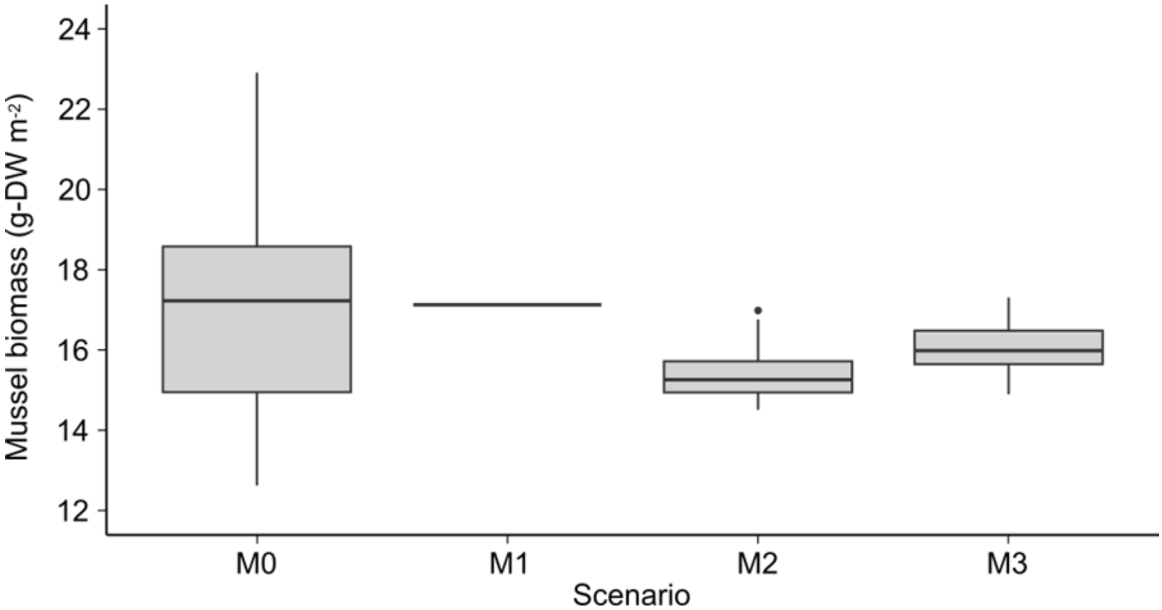

Figure 3.4.2. *Total biomass of mussels (g-DW m^{-2}) for each individual farm at time of harvest (31st December) for scenarios M0 (farms in all model elements, no feedback to biogeochemical model), M1 (single farm in pilot farm location), M2 (112 farms placed 343 m distant from one another), and M3 (55 farms placed 686 m distant from one another).*

"Funded by the European Union, grant agreement NO 101094065. Views and opinions expressed are however those of the author(s) only and do not necessarily reflect those of the European Union or CINEA. Neither the European Union nor the granting authority can be held responsible for them."

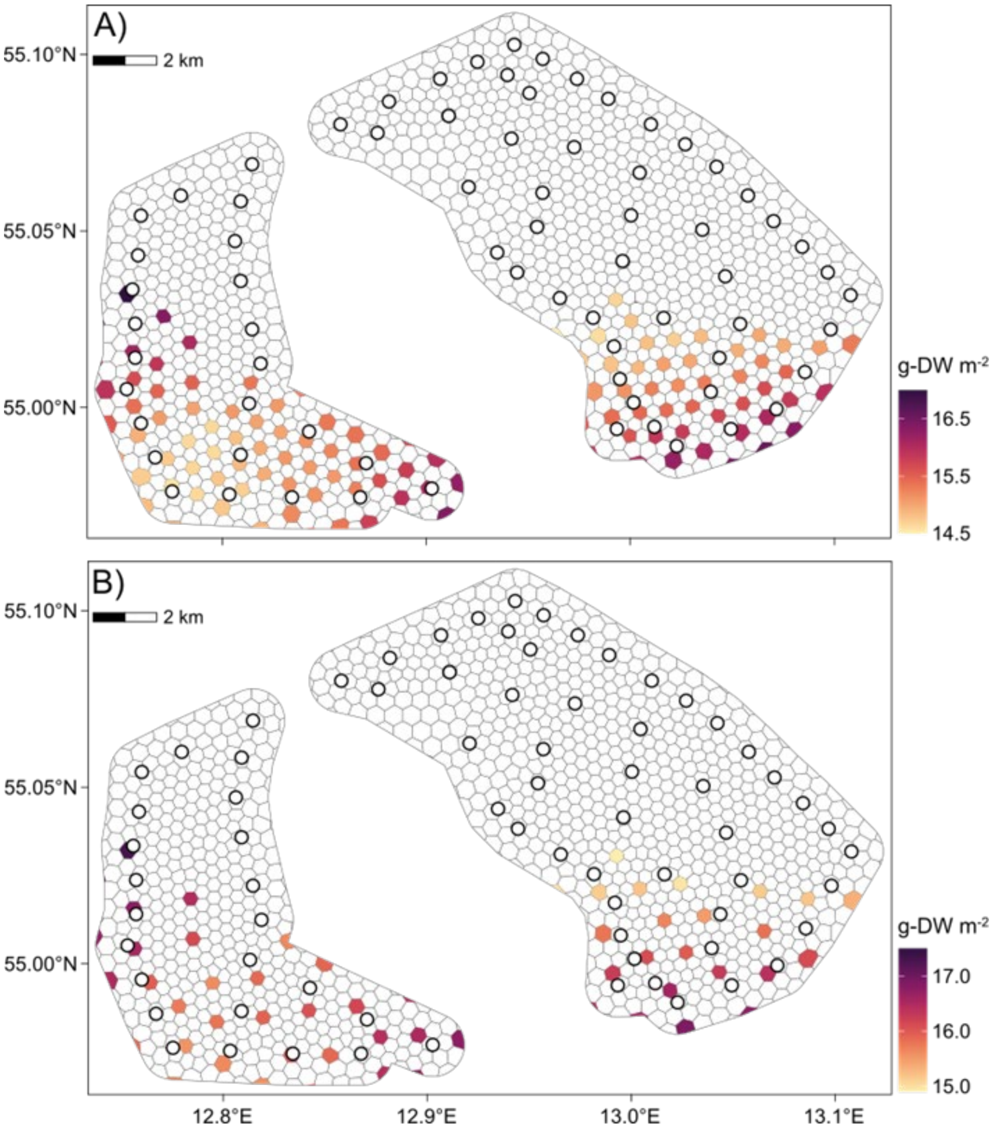

Figure 3.4.3. *Total biomass of mussels (g-DW m^{-2}) for each individual farm at time of harvest (31st December) for scenarios M2 (112 farms placed 343 m distant from one another), and M3 (55 farms placed 686 m distant from one another).*

"Funded by the European Union, grant agreement NO 101094065. Views and opinions expressed are however those of the author(s) only and do not necessarily reflect those of the European Union or CINEA. Neither the European Union nor the granting authority can be held responsible for them."

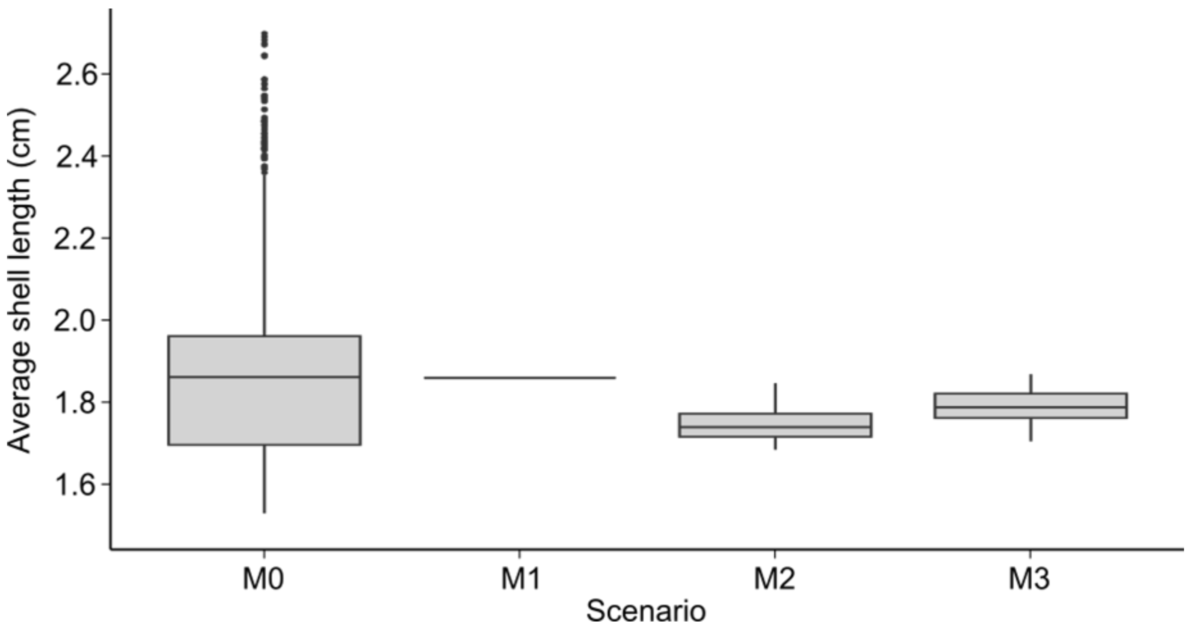

Figure 3.4.4. *Average shell length (cm) of mussels calculated across depth (1 – 5 m) for each individual farm at time of harvest (31st December) for scenarios M0 (farms in all model elements, no feedback to biogeochemical model), M1 (single farm in pilot farm location), M2 (112 farms placed 343 m distant from one another), and M3 (55 farms placed 686 m distant from one another).*

3.4.2 Kelp farming productivity

The maximum potential biomass of kelp (g-DW m^{-2}) from 0 – 15 m depth at time of harvest (1st June) for scenario K0 (the screening scenario) is displayed in Figure 3.3.2B. At the time of harvest (1st June) kelp biomass at the pilot farm location in Scenario K1 was 2.17 g-DW m^{-2} (Figure 3.4.3A). Average kelp biomass across farm locations at the time of harvest was also 2.17 ± 0.02 g-DW m^{-2} for both Scenario K2 (343 m distance between farms; Figure 3.4.3B) and Scenario K3 (686 m distance between farms; Figure 3.4.3C).

"Funded by the European Union, grant agreement NO 101094065. Views and opinions expressed are however those of the author(s) only and do not necessarily reflect those of the European Union or CINEA. Neither the European Union nor the granting authority can be held responsible for them."

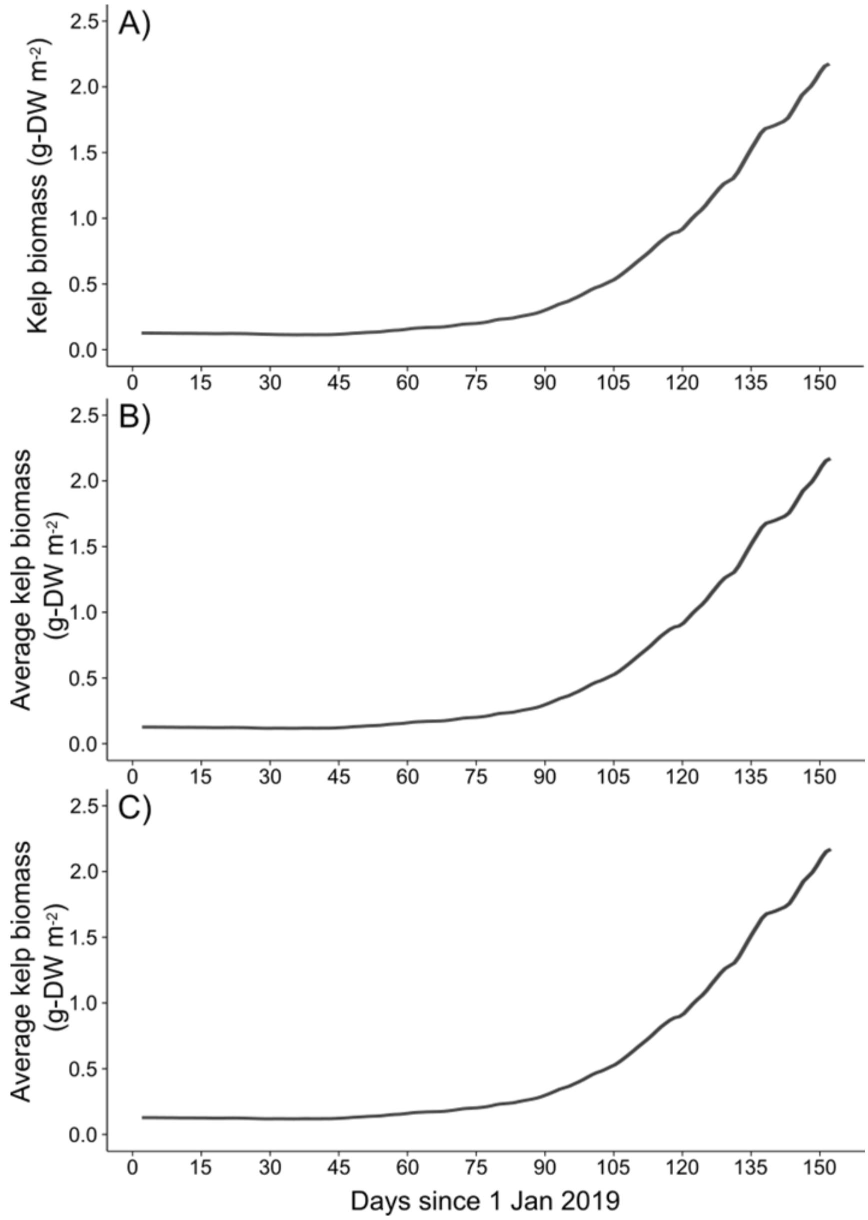

Figure 3.4.5. *Model results for total biomass of kelp (g-DW m*$^{-2}$*) from 1*st *January – 1*st *June for model scenarios K1, K2 and K3.* ***A)*** *Kelp biomass in scenario K1, where a single kelp farm was placed in the pilot farm location.* ***B)*** *Average kelp biomass of a single farm in scenario K2, where 112 farms were placed 343 m distant from one another.* ***C)*** *Average kelp biomass of a single farm in scenario K3, where 55 farms were placed 686 m distant from one another. In* ***B*** *and* ***C****, a shaded area indicates ± the standard deviation of the average value, however the standard error values are low enough that the shaded areas are not visible.*

There was no observable difference in kelp biomass (g-DW m^{-2}) per individual farm at the time of harvest between scenarios K2, where farms were placed 343 m distant from one another, and K3, where farms were placed 686 m distant from one another (Figure 3.4.4). This is likely due to the current model parameterization, in which biomass is driven by light and there is no influence of NO_3 limitation on kelp carbon biomass (only on N-reserves). This is actively being worked on and will be added to the kelp model in the next version.

"Funded by the European Union, grant agreement NO 101094065. Views and opinions expressed are however those of the author(s) only and do not necessarily reflect those of the European Union or CINEA. Neither the European Union nor the granting authority can be held responsible for them."

Kelp biomass in scenarios K2 and K3 was generally marginally lower than for scenario K0, where there was no feedback from the kelp model to the biogeochemical model.

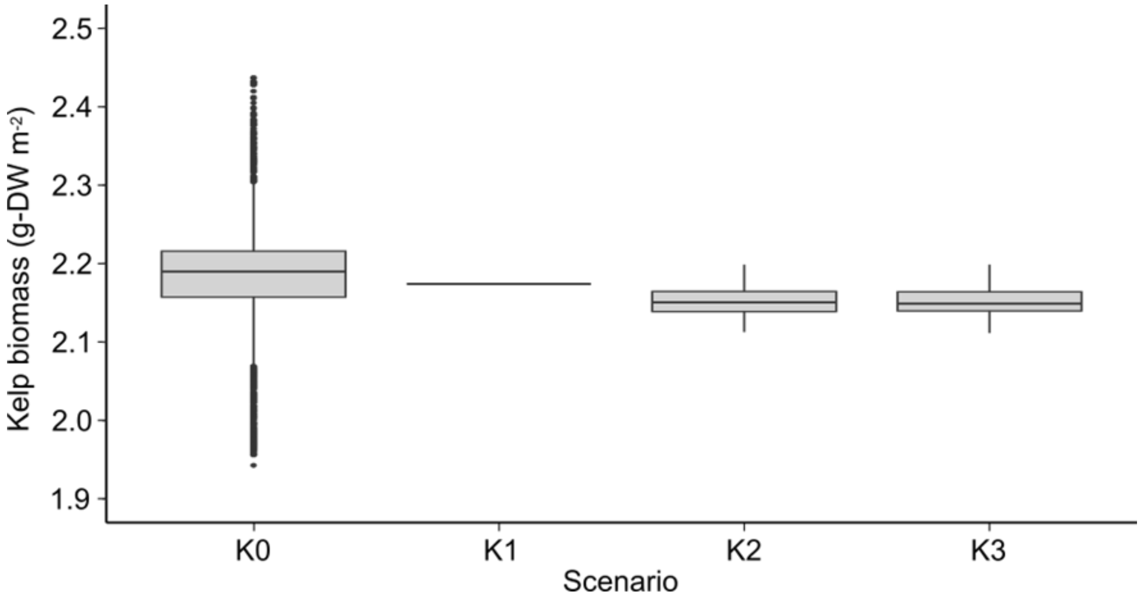

Figure 3.4.6. *Total biomass of kelp (g-DW m^{-2}) for each individual farm at time of harvest (1st June) for scenarios K0 (farms in all model elements, no feedback to biogeochemical model), K1 (single farm in pilot farm location), K2 (112 farms placed 343 m distant from one another), and K3 (55 farms placed 686 m distant from one another).*

3.4.3 Data description and structure

The data displayed above are contained within netCDF files. One netCDF file was created for each scenario, the names of which are displayed in Table 3.4.1. The data are unstructured and use UTM32 projection.

Table 3.4.1. *Filenames of the netCDF files containing data on farming potential for mussel and kelp aquaculture within Kriegers Flak Offshore Wind Farm.*

Scenario	Filename
M0	M0_case_study_B_KF_mussels.nc
K0	K0_case_study_B_KF_kelp.nc
M1	M1_case_study_B_KF_mussels.nc
K1	K1_case_study_B_KF_kelp.nc
M2	M2_case_study_B_KF_mussels.nc
K2	K2_case_study_B_KF_kelp.nc
M3	M3_case_study_B_KF_mussels.nc
K3	K3_case_study_B_KF_kelp.nc

"Funded by the European Union, grant agreement NO 101094065. Views and opinions expressed are however those of the author(s) only and do not necessarily reflect those of the European Union or CINEA. Neither the European Union nor the granting authority can be held responsible for them."

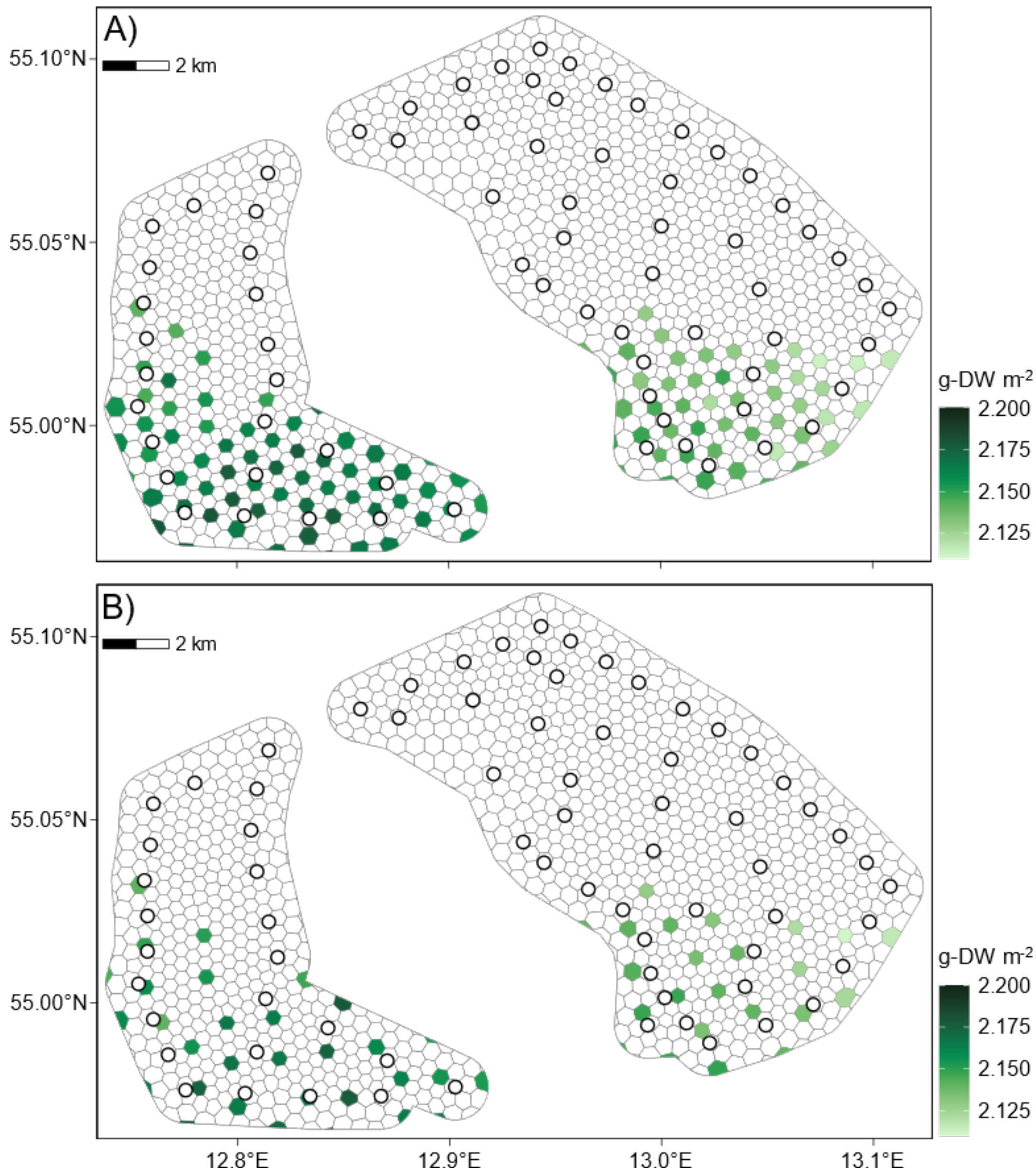

Figure 3.4.7. *Total biomass of kelp (g-DW m^{-2}) for each individual farm at time of harvest (1st June) for scenarios A) K2 (112 farms placed 343 m distant from one another), and B) K3 (55 farms placed 686 m distant from one another).*

"Funded by the European Union, grant agreement NO 101094065. Views and opinions expressed are however those of the author(s) only and do not necessarily reflect those of the European Union or CINEA. Neither the European Union nor the granting authority can be held responsible for them."

4. Case study C: Tagalaht Bay, Estonia

The Case Study at Tagalaht Bay in Estonia comprises a multi-use area with integrated multi-trophic aquaculture (IMTA) approach. Just within a few meters, the case study location hosts a fish farm (rainbow trout), and a multi-use plot holding a blue mussel farm and production units for seaweeds: *Ulva* and *Fucus* (Fig. 4.1).

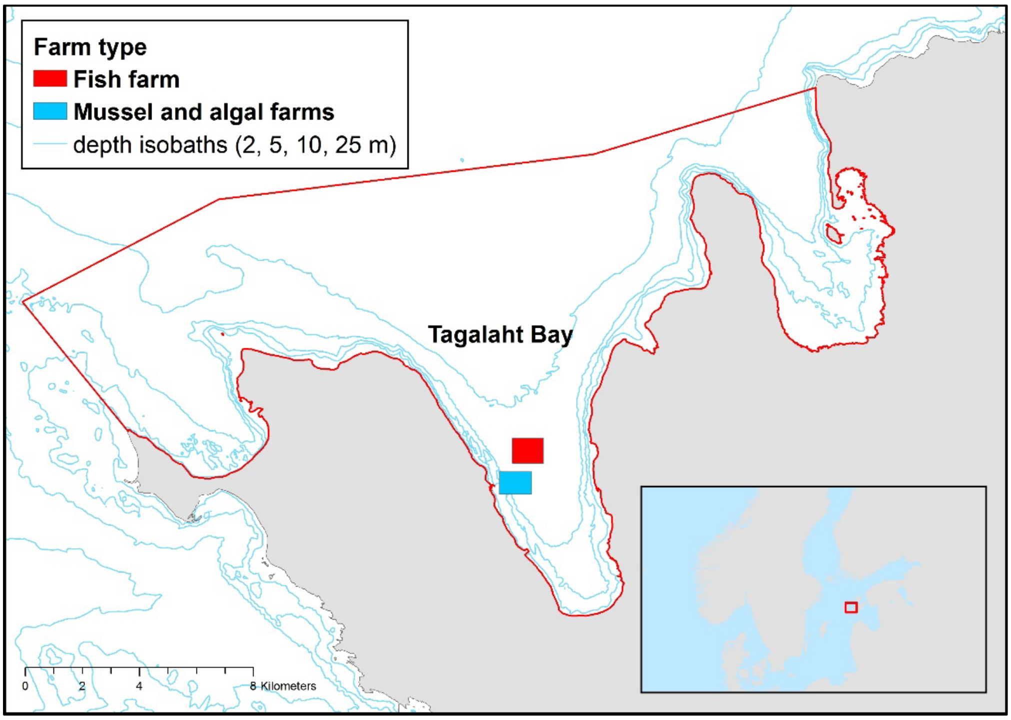

Figure 4.1. *Map of the Case Study area at Tagalaht Bay in Estonia*.

<u>*Rainbow Trout farm:*</u> The rainbow trout farm adjacent to the mussel farm in Tagalaht Bay consists of seven net cages, each 38 m in diameter, housing tens of thousands of fish (approx. 300 t production annually). Fish are introduced at 0.85 kg wet weight after being raised in a hatchery and are cultivated for six months (May–October). Feed is delivered via boats but cannot be distributed during storms (wave height >2 m), potentially affecting growth rates. Fish are fed with Blue Impact pellets (6 mm for smaller fish, 8 mm for larger fish), with nutrient emissions decreasing as fish grow due to the lower nitrogen (N) and phosphorus (P) content in larger pellets. Most phosphorus settles on the seabed as non-bioavailable hydroxyapatite, reducing its environmental impact.

<u>*Blue mussel farm:*</u> The test mussel farm in Tagalaht Bay (0.25 ha) uses a self-regulating system relying on larvae recruitment from wild populations. Mussels are cultivated on nets at 1–5 m depth, cleaned, and harvested by specialized machines (SmartFarm A/S) after a 1.5-year cycle from June to October of the following year. The farm has six 100 m long lines with a stocking density of ~40 million mussels.

<u>*Fucus seaweed farm:*</u> The test seaweed farm in Tagalaht Bay focuses on cultivating a local variety of *Fucus vesiculosus*, a naturally drifting form found on the seafloor, which is well-suited for cultivation in mesh cage setups. This variety is native to Estonia's coastal waters.

"Funded by the European Union, grant agreement NO 101094065. Views and opinions expressed are however those of the author(s) only and do not necessarily reflect those of the European Union or CINEA. Neither the European Union nor the granting authority can be held responsible for them."

Cultivation relies on harvested seaweed that is transported and set-up in farms where it is allowed to grow freely. The farm consists of a net cage structure floating on the surface, supported by a buoyant ring. The net is attached and kept stretched by a ballast ring, this allows *Fucus* to develop at a depth down to 1.5 meters, with an algal layer approximately 50 cm thick. Each farm unit covers an area of 6 m², and cultivation takes place from April to October.

4.1. Description of modeling approach

Tagalaht Bay is a small area, and the modeling approach in this pilot study focused specifically on the bay. For this case study, we used available data derived from large-scale ocean circulation and biogeochemical models to generate environmental conditions for the bay, including temperature, salinity, NO_3, wave conditions, current velocity, and Chl *a*. Input data were sourced from the Copernicus Marine Service, incorporating high-resolution outputs from models such as HIROMB-BOOS, BALMFC-ERGOM, and NEMO (https://data.marine.copernicus.eu/product/BALTICSEA_MULTIYEAR_PHY_003_011/services).

Despite the relatively high resolution of these models, their application to Tagalaht Bay remains coarse (~1.5 km resolution). In this task, population models developed for rainbow trout, mussels, and seaweed were applied to the available data for Tagalaht Bay to estimate potential production under realistic farming scenarios. Single-box simulations were performed for each model cell, and all simulations for each farm/species were run independently, assuming no other activities occurred in the area.

Rainbow Trout farm: The DEB parameters used for *O. mykiss* were based on the parameter estimation published in the AmP database (2022), Kooijman et al. (2017) and location-specific data in a commercial farm in Tagalaht Bay. The parameters of the temperature correction function $T_A, T_H, T_{AH}, T_L, T_{AL}$ were updated using growth data at the upper thermal tolerance of the species (Chen et al., 2015).

Zero-variate datasets included ages, DW of tissue or wet weights of tissue of all important life stages (hatch, birth, puberty) (From & Rasmussen, 1991; Davidson et al., 2014). Ultimate life span, ultimate length, ultimate wet weight, and maximum reproduction rate were also included (Tyler et al., 1996; Fishbase, 2022). Univariate datasets included hatching time at different temperatures (Velsen, 1987), growth of embryos (Ninness et al., 2006), growth of fingerlings (Yanik et al., 2002), oxygen consumption (Wieser, 1985; Lauff & Wood, 1996; Kieffer et al., 1998), and measurements of wet weight during starvation (Sumpter et al., 1991; Weatherley & Gill, 1981). To get location-relevant information, unpublished growth data was included from 4 net pens of a commercial farm in Estonia (Redstorm Ltd.). The feeding of cage 4 was lower ($f = 0.65$) than the other cages ($f = 0.7$) due to suppressed appetite (personal comment from farmer) and food availability was considered constant (Stavrakidis-Zachou et al., 2019). The temperature profile at the site was based on *in situ* measurements using a calibrated Optode-type oxygen sensor (Aanderaa Instruments) that also records temperature. Validation was done by estimating fish weights and feed efficiency ratios based on the feeding rates published by Davidson et al., (2014).

"Funded by the European Union, grant agreement NO 101094065. Views and opinions expressed are however those of the author(s) only and do not necessarily reflect those of the European Union or CINEA. Neither the European Union nor the granting authority can be held responsible for them."

Blue mussel farm: The DEB model parameters were based on Roberts & Kooijman (2019) and were complemented with existing evidence on important life history events and metabolic characteristics. Thirteen uni- and multivariate datasets were included in the estimation process and included: total wet weight of mussels (Veber, 1998), clearance and biodeposition rates collected at different locations across the Baltic Sea (Kotta et al., 2005; Lauringson et al., 2009). Mussel growth (DW) was monitored during lab experiments at salinities of 7 and 20, an average Chl a concentration of 3.8 µg L^{-1} and a temperature of 10.8 °C (Riisgård et al., 2013). The elementary composition of the organic compounds and the shell (defined in the model as a part of structure) was defined based on measurements of N and P content in mussel tissue (Buer et al., 2020b), total mussel DW (Kotta et al., 2020) and total mussel wet weight (Petersen & Loo, 2004; Buer et al., 2020b).

Fucus seaweed farm: A different modelling approach was used for *Fucus*. In this case a simple mechanistically founded model was applied. This model was derived from the *Saccharina* model used in Pilot B and follows the same set of assumptions. This *Fucus* model includes several extensions to accommodate the unique data types available and the biological differences specific to the species. we did not fit a salinity scaling function, while salinity in the Baltic Sea is low, this model was already calibrated for low salinity and the data available did not cover a salinity gradient large enough to calibrate a scaling function for salinity (Talagaht bay salinity ranges from 5.5 to 6.5). However, we parameterized and calibrated scaling functions affecting the daily increment of biomass produced by the model to account for the effect of temperature (which ranges between 0 and 21 ˚C. in Tagalaht bay) and nitrates. The data used to calibrate this model suggested the need for this scaling function to properly describe the growth of *Fucus* during the production cycle in Tagalaht bay. In this manner the equation in 3.1.4 becomes:

$$\Delta M = T_f \times \left[\left(\alpha \times N_f\right) \times M_{CH_2O} \times I_{abs} - (r \times M)\right]$$

Where T_f is a scaling factor for temperature effect affecting both photosynthesis and respiration and therefore scaling growth and N_f is a scaling factor for photosynthesis to describe the limitation by the availability of NO_3 without affecting dark respiration.

The parameterization of these scaling function are as follows: for temperature, we used the Arrhenius concept as described by Kooijman 2010 for Dynamic Energy Budget models to describe the effect of temperature on the growth rate of *Fucus*. We used:

$$T_f = exp\left\{\frac{T_A}{T_1} - \frac{T_A}{T}\right\} \cdot \left(1 + exp\left\{\frac{T_{AL}}{T} - \frac{T_{AL}}{T_L}\right\} + exp\left\{\frac{T_{AH}}{T_H} - \frac{T_{AH}}{T}\right\}\right)^{-1}$$

Where T_A, T_{AL}, T_{AH} are the Arrhenius temperatures at the optimal range, beyond the lower threshold and beyond the higher threshold respectively and T_L, T_H are the lower and higher temperature thresholds (see Kooijman et al. 2010).

"Funded by the European Union, grant agreement NO 101094065. Views and opinions expressed are however those of the author(s) only and do not necessarily reflect those of the European Union or CINEA. Neither the European Union nor the granting authority can be held responsible for them."

For nitrates, we modeled the limitation by nitrogen as a function of NO_3 concentration in the water (*mmol/m³*). We parameterized it as a resource functional response following a Hollings type II function.

$$N_f = \frac{[NO_3]}{[NO_3] + k_N}$$

Where k_N is the half saturation with same units as the concentration of NO_3 ($mmol/m^3$).

Model was calibrated using datasets of *Fucus* growth under different environmental conditions with ranges of salinity, temperature, nutrients and light relevant to the Baltic Sea region. No significant effect of salinity or phosphates on growth were encountered in these datasets and therefore only nitrate, temperature and light are used as input variables for this model.

4.2. Model validation

Trout and blue mussel model validations were done against empirical datasets consisting of growth and other traits under contrasting environmental conditions. In total 34 and 32 datasets, for trout and mussel respectively were used for model validation. In both cases, model mean relative error (MRE) for all datasets was below 0.2 (more details in Kotta et al. 2022).

For the calibration and validation of the *Fucus* model we used data from experimental farming. In late 2023, AquaVerde Ltd established the first offshore seaweed farm in the low-salinity region of the Baltic Sea at the multiuse pilot C. Initial trials were conducted as part of the HORIZON project AlgaeProBanos, examining how different farm configurations and dimensions influenced both farm stability and seaweed growth. Based on these findings, an optimal setup was chosen, and from April to October 2024, the test farm successfully cultivated the drifting form of *Fucus vesiculosus*. Data on daily growth, biomass and photosynthesis along with key environmental parameters, including water temperature, light intensity, water velocity, turbidity, salinity, and wave dynamics, were monitored using underwater autonomous instruments throughout production. The *fucus* model performed well during the summer season, slightly underestimating growth during the colder spring months, and did not account for grazing losses starting mid-August (Figure 4.2.1). However, these issues will be addressed in the next version.

"Funded by the European Union, grant agreement NO 101094065. Views and opinions expressed are however those of the author(s) only and do not necessarily reflect those of the European Union or CINEA. Neither the European Union nor the granting authority can be held responsible for them."

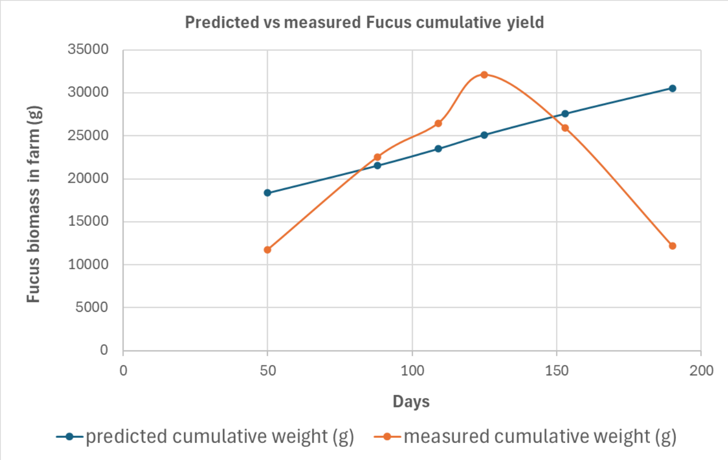

Figure 4.2.1. Model comparison of *Fucus* growth with measurements over time.

4.3. Run scenarios

We run realistic farm settings for rainbow trout, blue mussels and fucus seaweed. The scenarios run are the set-ups used by the activity at the study case in Tagalaht Bay (Figure 4.3.1, orange dot in maps).

Aquaculture is increasingly regarded as a promising solution for meeting the growing global demand for fish, but this potential can only be realized if the industry reduces its reliance on wild-caught fish in feeds and mitigates its environmental impacts. Integrated multi-trophic aquaculture (IMTA), the practice of cultivating extractive species like macroalgae and bivalves alongside finfish, offers a potential pathway for improving environmental sustainability. By actively up-taking and assimilating dissolved nutrients released from finfish farms, these low-trophic-level organisms help remove excess nutrients from the ecosystem once they are harvested.

This case study investigated the potential of mussels and macroalgae to serve as a bioremediation tool at finfish farms in the eutrophic Baltic Sea region. We run Dynamic Energy Budget (DEB) models for blue mussels (*Mytilus edulis/trossulus*) and rainbow trout (*Oncorhynchus mykiss*) and a mechanistic dynamic model for *Fucus vesiculosus* with a regional hydrodynamic-biogeochemical model to assess how mussel and macroalgae farming could compensate for nutrient discharges from finfish farms and what is the potential yield of both species in the area.

The aim of this pilot case was to analyze the potential use of blue mussels and macroalgae to mitigate the negative environmental impacts of fish farming, as discussed in Kotta et al. (2023). These scenarios do not simulate an IMTA set-up where interactions between the different farming activities and the environment are fully coupled. In this study case the run scenarios simulated the potential of each farm activity individually in the region with the aim to assess the production potential of each species and the fluxes for nutrients. In this deliverable only data on production potential are provided with the analyses of data on nutrients being part of D3.2 on ecosystem services. In D3.2. the IMTA potential of this set-up will be assessed.

"Funded by the European Union, grant agreement NO 101094065. Views and opinions expressed are however those of the author(s) only and do not necessarily reflect those of the European Union or CINEA. Neither the European Union nor the granting authority can be held responsible for them."

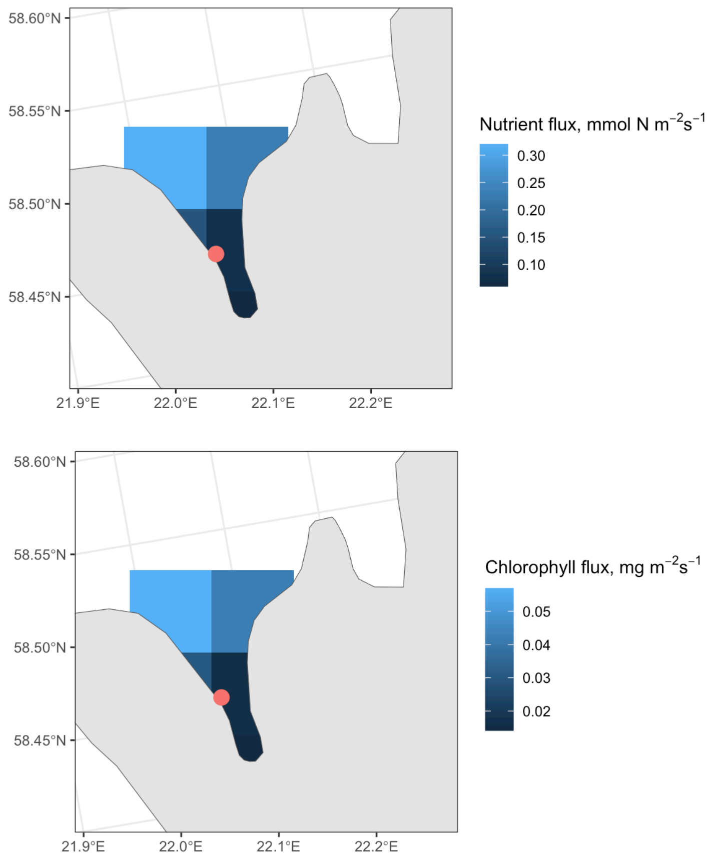

Figure 4.3.1. *Annual mean food and nutrient flux within the Tagalaht Bay. Top: Average nutrient flux (mmol NO_3 m^{-2} s^{-1}). Bottom: Average food flux (mg Chl* a *m^{-2} s^{-1}). Orange dot is the location of the multiuse study area (pilot C).*

In this study case there is only one scenario run for each species, corresponding with the set-up running at the pilot. More specifically for each farm/species:

Finfish farming is fed farming and for the simulation we used the characteristics of the selected fish feed pellets to assess the fluxes of nutrients between the farm and the environment. Farm set-up was done using a realistic density with 70000 individuals and the simulations were run from the 1st of May to 21st of October. This is the production cycle at the area (Figure 4.3.1)

"Funded by the European Union, grant agreement NO 101094065. Views and opinions expressed are however those of the author(s) only and do not necessarily reflect those of the European Union or CINEA. Neither the European Union nor the granting authority can be held responsible for them."

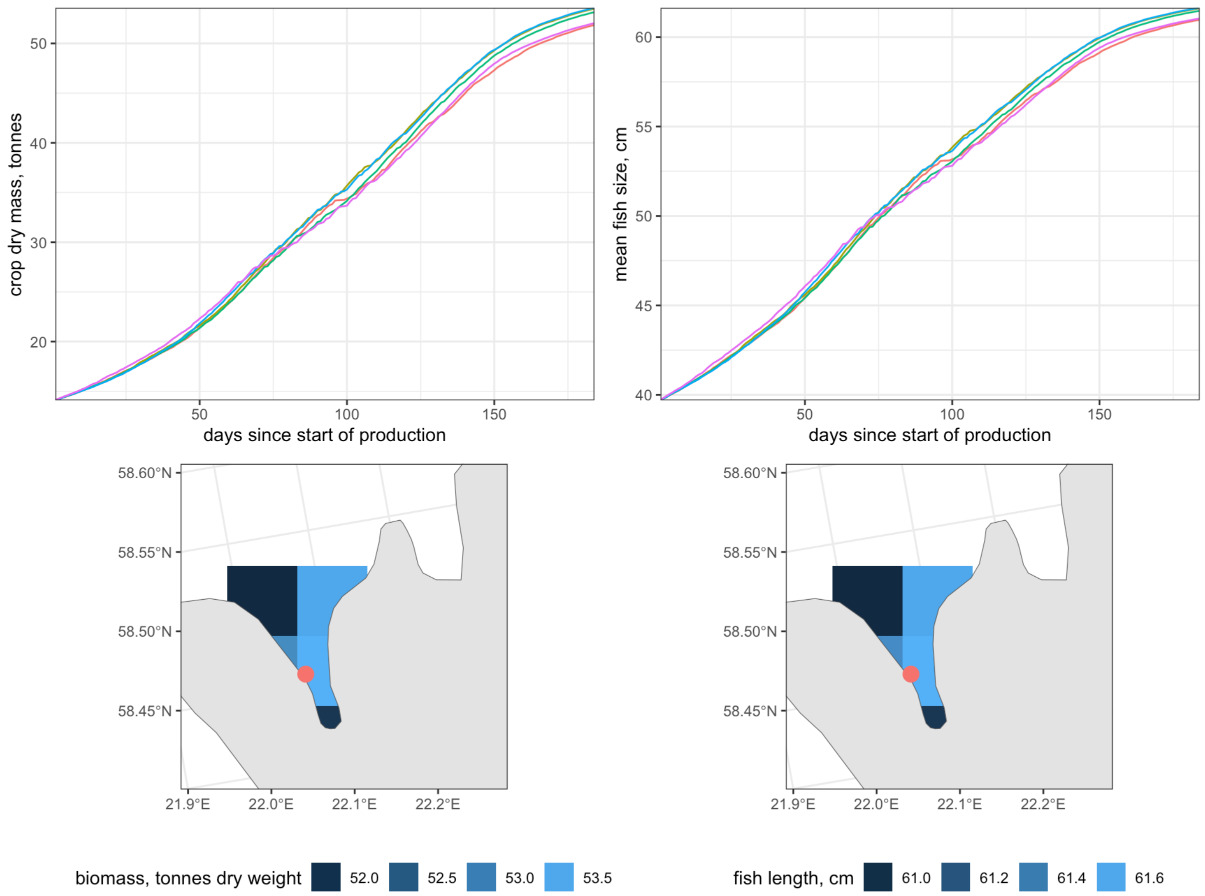

Figure 4.3.2. *Rainbow trout growth and biomass production (on the same farm setting) at Tagalaht bay. Each line in the top row plots represent one of the grid cells showing in the bottom maps. Orange dot in map shows the multiuse pilot location.*

For the blue mussel, the model was run under a realistic scenario involving a test farm with a population of 40 million individuals, distributed across six 100-meter-long lines. Blue mussel farms were run from 1st of June to the 21st of October of a year later (Figure 4.3.3). In this study case no differentiation is made between mitigation and human consumption mussels, that is because obtaining commercial size mussels is not feasible in this site due to low salinity.

"Funded by the European Union, grant agreement NO 101094065. Views and opinions expressed are however those of the author(s) only and do not necessarily reflect those of the European Union or CINEA. Neither the European Union nor the granting authority can be held responsible for them."

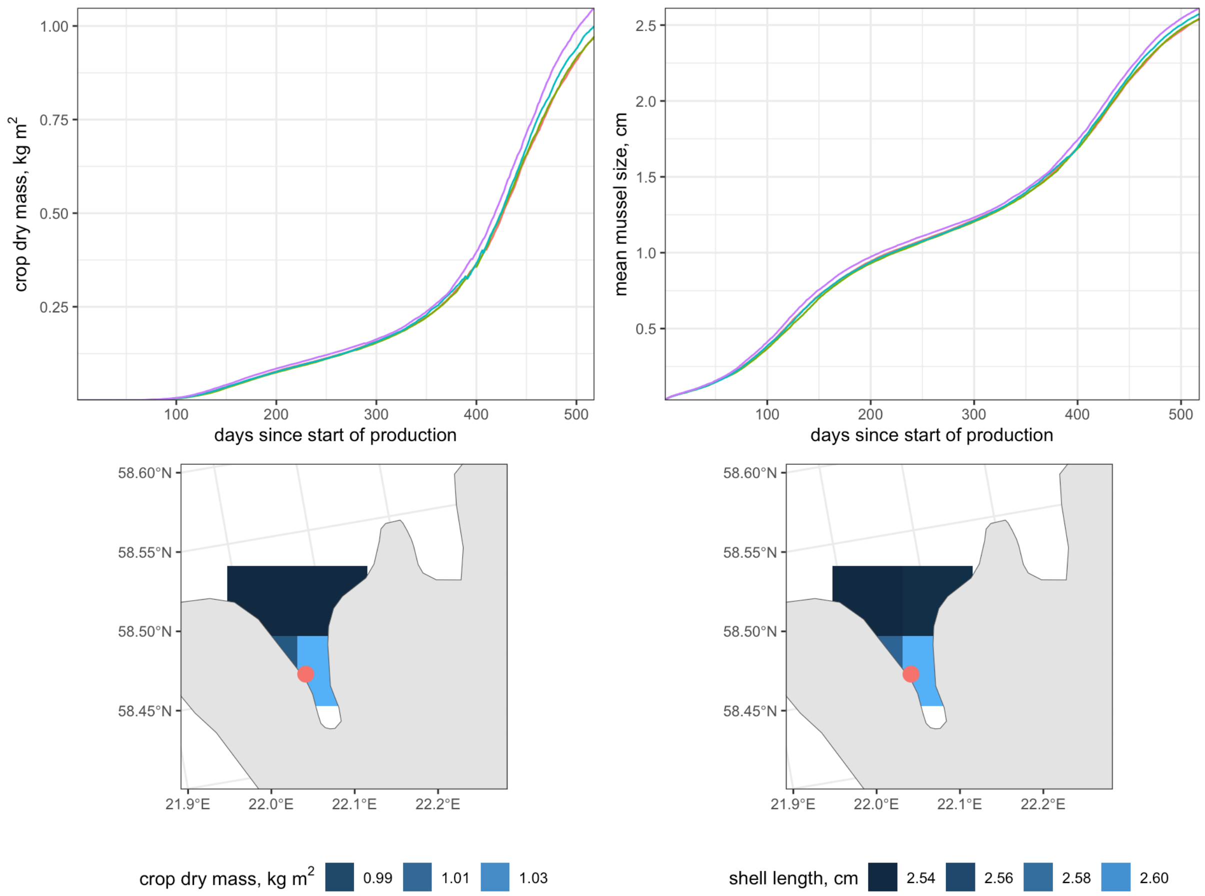

Figure 4.3.3. *Mussel production potential (DW per m²) and growth in shell length (on the same farm setting) at Tagalaht bay. Each line in the top row plots represent one of the grid cells showing in the bottom maps.*

The *Fucus* model was applied to a *Fucus* production set-up consisting of one net cage with a surface area of 6 m². An initial biomass of 10 kg of DW of algae is used in the modelling scenario. Simulation takes place from April to October.

4. Data description and structure

Delivered dataset contains the model runs for all 5 grid cells represented in figures 4.3.1-4. These are the model runs for the three species with farm set-ups as explained in 4.3. Datasets contains stock as wet mass, dry mass and length for both rainbow trout and blue mussel. For *Fucus* the output contains dry mass for the crop and daily growth. Additionally, environmental conditions used for model forcing are included in each dataset. An additional dataset is provided with the nitrogen and Chl *a* fluxes resulting from calculations using the forcing variables obtained from Copernicus Marine Service.

"Funded by the European Union, grant agreement NO 101094065. Views and opinions expressed are however those of the author(s) only and do not necessarily reflect those of the European Union or CINEA. Neither the European Union nor the granting authority can be held responsible for them."

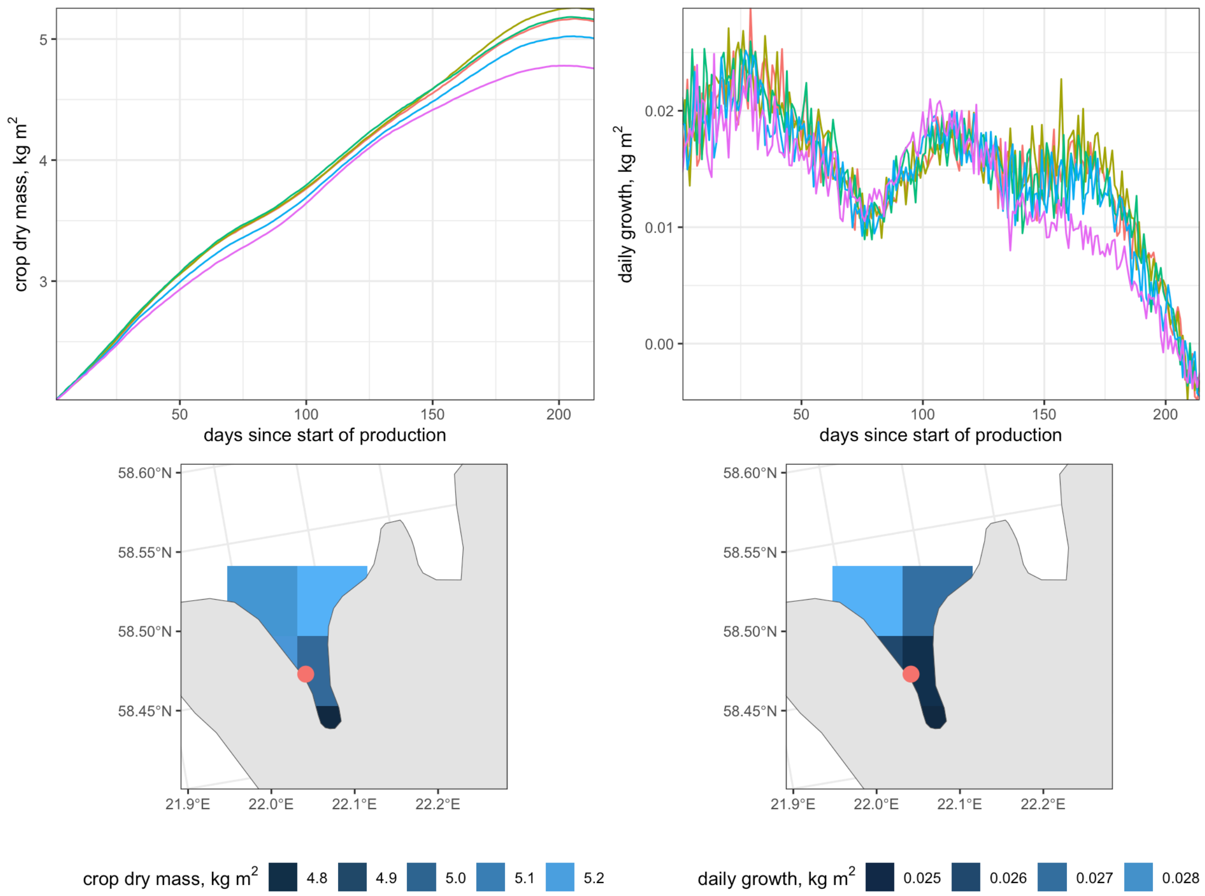

Figure 4.3.4. *Macroalgae production potential (DW per m^2) and daily growth (on the same farm setting, one cage of $6m^2$) at Tagalaht bay. Each line in the top row plots represent one of the grid cells showing in the bottom maps.*

Table 4.4.1. *Filenames of the netCDF files containing data on farming potential trout, mussel and fucus aquaculture, and a dataset containing the calculated nutrient and chlorophyll a fluxes within Tagalaht bay, Estonia.*

Scenario	Filename
Trout	trout_case_study_C_TB.nc
Mussel	mussel_case_study_C_TB.nc
Fucus	fucus_case_study_C_TB.nc
Fluxes	fluxes_case_study_C_TB.nc

"Funded by the European Union, grant agreement NO 101094065. Views and opinions expressed are however those of the author(s) only and do not necessarily reflect those of the European Union or CINEA. Neither the European Union nor the granting authority can be held responsible for them."

5. Summary

Ecosystem models coupled with low trophic aquaculture models (mussels and seaweed) were developed and validated against available measurements at the three OLAMUR case study sites. The models were applied to estimate the potential harvest and provide data sets for other WPs. The sites varied in environmental properties with highest salinity at site A in the German Bight, and very low salinity in the Baltic Sea at site B (Kriegers Flak) and C (Tagalaht bay). Fluxes of Chl *a* and nutrients supplying the aquaculture farms were highest in the German Bight followed by Kriegers Flak, and Tagalaht bay (Table 5.1).

Blue mussels could be produced at each site. The mussel farm at site C is already well established and production has been optimized to achieve a high harvest of 1000 g-DW m^{-2} despite the low salinity. At the two other sites, information of mussel growth from WP1 is still lacking. Especially knowledge of individual mussel biomass and the number of mussels per m^3 of farm volume will be useful to access the full harvest potential. The models here used a conservative approach of rather low mussel density in the farms, and we expect that harvest potential will be higher in the next version of model runs.

Sugar kelp was found to be very sensitive to low salinity showing low growth rates and farming must be considered unsuitable for Kriegers Flak based on both measurements and modelling. It would probably be more ideal to grow sugar kelp at higher salinities, e.g., offshore at site A in the German Bight.

Fucus showed the highest harvest potential among the tested species and will be worth cultivating. This represents the first successful case of seaweed cultivation in the low-salinity environment of the Baltic Sea. The only challenge was the strong grazing on *Fucus* observed later in the season, which could be managed with proper strategies.

	Site A German Bight	**Site B Kriegers Flak**	**Site C Tagalaht bay**
Salinity (psu)	29.7-34.3	7.5-8.5	5.5-6.5
Chl a flux (mg-m^{-2} s^{-1})	0.95-1.20	0.15-0.30	0.02-0.05
Nitrogen flux (mmol m^{-2} s^{-1})	-	0.7-1.5	0.1-0.3
Mussel harvest (g-DW m^{-2})	50-350	15-17	1000
Sugar kelp harvest (g-DW m^{-2})	-	2.2	-
***Fucus* harvest (g-DW m^{-2})**	-	-	4800-5200

Table 5.1. Summary of the model estimates of Chl *a* and nutrient fluxes and harvest potential at the three sites.

"Funded by the European Union, grant agreement NO 101094065. Views and opinions expressed are however those of the author(s) only and do not necessarily reflect those of the European Union or CINEA. Neither the European Union nor the granting authority can be held responsible for them."

6. References.

Buer, A-L., Maar, M., Nepf, M., Ritzenhofen, L., Dahlke, S., Friedland, R., Krost, P., Peine, F., & Schernewski, G. (2020). Potential and feasibility of *Mytilus* spp. farming along a salinity gradient. *Frontiers of Marine Science*, *7*. https://doi.org/10.3389/fmars.2020.00371

Bruggeman, J., and Bolding, K. (2014). A general framework for aquatic biogeochemical models. *Environmental modelling and software*, *61*, 249-265. https://doi.org/10.1016/j.envsoft.2014.04.002

Daewel, U., and Schrum, C. (2013). Simulating long-term dynamics of the coupled North Sea and Baltic Sea ecosystem with ECOSMO II: Model description and validation. *Journal of Marine Systems*, *119*, 30-49. https://doi.org/10.1016/j.jmarsys.2013.03.008

Holst, N., Boderskov, T., & Bruhn, A. (in review). A simple growth model of *Saccharina latissima* cultivated in Scandinavia: Theoretical and practical implications.

Kotta, J.; Stechele, B.; Barboza, F.R.; Kaasik, A.; Lavaud, R. 2023. Towards environmentally friendly finfish farming: A potential for mussel farms to compensate fish farm effluents. Journal of Applied Ecology, 60, 1314–1326. https://doi.org/10.1111/1365-2664.14422

Kaspar, F., Niermann, D., Borsche, M., Fiedler, S., Keller, J., Potthast, R., Rösch, T., Spangehl, T., and Tinz, B.: Regional atmospheric reanalysis activities at Deutscher Wetterdienst: review of evaluation results and application examples with a focus on renewable energy, Adv. Sci. Res., 17, 115–128. https://doi.org/10.5194/asr-17-115-2020, 2020

Maar, M., Bolding, K., Petersen, J. K., Hansen, J. L., and Timmermann, K. (2009). Local effects of blue mussels around turbine foundations in an ecosystem model of Nysted off-shore wind farm, Denmark. *Journal of Sea Research*, *62*(2-3), 159-174. https://doi.org/10.1016/j.seares.2009.01.008

Maar, M., Larsen, J., Butenschön, M., Kristiansen, T., Thodsen, H., Taylor, D., & Schourup-Kristensen, V. (2024). Impacts of climate change on water quality, benthic mussels, and suspended mussel culture in a shallow, eutrophic estuary. *Heliyon*, *10*(3). https://doi.org/10.1016/j.heliyon.2024.e25218

Maar, M., Larsen, J., Schourup-Kristensen, V., & Taylor, D. (2023). Nutrient extraction and ecosystem impact by suspended mussel mitigation cultures at two contrasting sites. *Science of the Total Environment*, *888*. https://doi.org/10.1016/j.scitotenv.2023.164168

Pein, J., Eisele, A., Sanders, T., Daewel, U., Stanev, E. V., Van Beusekom, J. E., Staneva, J. and Schrum, C. (2021). Seasonal stratification and biogeochemical turnover in the freshwater reach of a partially mixed dredged estuary. *Frontiers in Marine Science*, *8*, 623714. https://doi.org/10.3389/fmars.2021.623714

Pein, J., Staneva, J., Mayer, B., Palmer, M. D., and Schrum, C. (2023). A framework for estuarine future sea-level scenarios: Response of the industrialised Elbe estuary to projected mean sea level rise and internal variability. *Frontiers in Marine Science*, *10*, 1102485. https://doi.org/10.3389/fmars.2023.1102485

Pein, J., Staneva, J. (2024). Eutrophication hotspots, nitrogen fluxes and climate impacts in estuarine ecosystems: A model study of the Odra estuary system. *Ocean Dynamics* **74**, 335–354. https://doi.org/10.1007/s10236-024-01607-w

"Funded by the European Union, grant agreement NO 101094065. Views and opinions expressed are however those of the author(s) only and do not necessarily reflect those of the European Union or CINEA. Neither the European Union nor the granting authority can be held responsible for them."

Radach, G., & Moll, A. (2006). Review of three-dimensional ecological modelling related to the North Sea shelf system. Part II: Model validation and data needs, in: Gibson, R. N., Atkinson, R. J. A., & Gordon, J. D. M. (Eds.), *Oceanography and Marine Biology. An Annual Review*, *44*, p. 1-60.

Rennau, H., Schimmels, S., & Burchard, H. (2012). On the effect of structure-induced resistance and mixing on inflows into the Baltic Sea: A numerical model study. *Coastal Engineering*, *60*, p. 53-68. https://doi.org/10.1016/j.coastaleng.2011.08.002

Schrum, C., Alekseeva, I., and John, M. S. (2006). Development of a coupled physical–biological ecosystem model ECOSMO: part I: model description and validation for the North Sea. *Journal of Marine Systems*, *61*(1-2), 79-99. https://doi.org/10.1016/j.jmarsys.2006.01.005

Taylor, D., Larsen, J., Buer, A-L., Friedland, R., Holbach, A., Petersen, J. K., Nelsen, P., Ritzenhofen, P., Saurel, C., & Maar, M. (2021). Mechanisms influencing particle depletion in and around mussel farms in different environments. *Ecological Indicators*, *122*. https://doi.org/10.1016/j.ecolind.2020.107304

Zhang, Y. J., Ye, F., Stanev, E. V., and Grashorn, S. (2016). Seamless cross-scale modeling with SCHISM. *Ocean Modelling*, *102*, 64-81. https://doi.org/10.1016/j.ocemod.2016.05.002

"Funded by the European Union, grant agreement NO 101094065. Views and opinions expressed are however those of the author(s) only and do not necessarily reflect those of the European Union or CINEA. Neither the European Union nor the granting authority can be held responsible for them."

“Funded by the European Union, grant agreement NO 101094065. Views and opinions expressed are however those of the author(s) only and do not necessarily reflect those of the European Union or CINEA. Neither the European Union nor the granting authority can be held responsible for them.”